8-2021

GABAergic-Related Pathology in the Anterior Cingulate Cortex of Postmortem Human Brain Tissue in Autism Spectrum Disorder

Gethien Andrew
East Tennessee State University

GABAergic-Related Pathology in the Anterior Cingulate Cortex of Postmortem Human Brain Tissue in Autism Spectrum Disorder

---

A thesis

presented to

the faculty of the Department of Biomedical Sciences

East Tennessee State University

In partial fulfillment

of the requirements for the degree

Master of Science in Biology, Biomedical Sciences

---

by

Gethein Andrew

August 2021

Dr. Michelle Chandley, Chair

Dr. Jonathan Peterson

Dr. Diego Rodriguez-Gil

Keywords: ASD, glutamate, GABAergic, immunoblotting, LCM, Anterior Cingulate Cortex

ABSTRACT

GABAergic-Related Pathology in the Anterior Cingulate Cortex of Postmortem Human Brain Tissue in Autism Spectrum Disorder

by

Gethein Andrew

The anterior cingulate cortex (ACC) is part of the cognitive and emotional brain circuitry that mediates social interaction. Imbalances between inhibitory, GABAergic neurons, and excitatory, glutamatergic neurons, in this region are essential to brain circuity during social responses and are thought to be involved with behaviors associated with autism spectrum disorder (ASD). Enriched cell populations of glutamatergic neurons, obtained through laser capture microdissection, were used for gene expression studies of GABAergic receptors (GABRA1, GABRA4, and GABBR1). Additionally, proteins that impact GABAergic synapses (Spinophilin, CPLX1, mTOR, IGF1R, PSD95, PARP1) were investigated using Western Blotting with punch-dissected homogenate brain tissue from ACC and frontal cortical brain regions. No significant differences in gene expression nor protein were identified between ASD and control brain donors. Evidence of GABAergic synaptic pathology was not found; however, future studies of alternative GABAergic markers and increased study numbers are needed to confirm these findings in ASD human tissue.

DEDICATION

In hopes that my research makes a difference, I would like to dedicate this to the research scientists who come after me. May my data collection help them advance their own projects and bring a better understanding to the world of Autism Spectrum Disorder.

ACKNOWLEDGEMENTS

To Dr. Michelle Chandley, the most hardworking and compassionate Principal Investigator, I would like to express my most sincere gratitude for allowing me a place in your laboratory and for always encouraging me to do my best work because you believed in my ability to complete the task at hand. Your mentorship has allowed me to gain techniques, knowledge, and confidence in myself and my potential to succeed. Thank you for introducing me into the world of Neuro, a passion for a career you helped to spark.

For help and support during this master's thesis research I would like to thank my faculty committee consisting of: Dr. Michelle Chandley, Dr. Jonathan Peterson, and Dr. Diego Rodriguez-Gil for their patience and advice over the years. They encouraged me to broaden my scope of learning and reach my peak potential of curiosity to explore all aspects of the project for a well-rounded educational experience.

A thank you to my parents who have never failed to support my dreams. I would not have set as many goals for myself if I did not have you both to tell me I should.

Finally, and arguably the most important, a thank you to all the tissue donors who solidified my ability to start this research. Without your donation to science little progress could be made in the field of developmental and cellular neuroscience. You have each stayed in my thoughts and your family in my prayers.

TABLE OF CONTENTS

LIST OF TABLES

LIST OF FIGURES

CHAPTER 1. INTRODUCTION

Autism Spectrum Disorder

Autism Spectrum Disorder (ASD) is a term coined in 1943 to name a neurodevelopmental disorder that affects human beings across the globe regardless of racial, ethnic, and socio-economic boarders. Autism is considered a spectrum disorder meaning that individuals with the disorder can have a very heterogenous symptom presentation i.e. complete lack of verbal communication or mildly impaired verbal skills. Changes made to the fifth edition of the Diagnostic and Statistical Manual of Mental Disorders (DSM-5) indicate the previous four distinct disorders including classic autism, Asperger's disorder, childhood disintegrative disorder, or pervasive developmental disorder are now blanketed under the term "autism spectrum disorder". [1] The disorder now affects 1 in 54 children in the United States with rates as high as 1 in 34 in males.[2] The economic burden of ASD in the U.S. alone is approaching ten billion annually. This cost is related to the nature of the disorder including a diagnosis before the age of three and needing lifelong services. Comorbidities such as intellectual disabilities that need special education classes and safe spaces to socialize are necessary and costly for families. [3]

Twin Studies

Currently, no effective pharmacological treatments exist to prevent, slow, or cure ASD increasing the urgency for understanding the pathobiology and progression of this disorder. Ill-defined pathophysiology and the lack of molecular markers of ASD translates to a purely behavioral diagnosis. The discovery of molecular markers by genetic studies or protein markers for ASD could lead to development of diagnostic methods and novel treatments. Genetics have been implicated in the development of ASD for over a decade which has led to several genetic and genomic approaches to provide evidence of the disruption of biological pathways. Some of

the most conclusive genetic studies of ASD use monozygotic (MZ) and dizygotic (DZ) twins where MZ twins share 100% of their genetic material while DZ share significantly less, but both MZ and DZ share the same *in-utero* environment. Comorbid rates of approximately 36 to 95% was found in MZ twin pairs providing support for a genetic etiology of ASD.[4,5]

Genetic Findings Associated with ASD

Genetics are likely involved in the etiology of ASD. Proband studies in ASD patients and families using blood and urine indicate that first-degree relatives have an increased risk for autism when certain variants are present such as Fragile X which is caused by de novo DNA mutations. [5,6] Banding pattern analyses revealed that 12-20% of the ASD probands exhibited a lesser variant, a gene variant that is more rare, which suggests autism etiology likely involves several genes that lead to the observed phenotype.[5,7] A recent large-scale exome sequencing analysis using ASD patients revealed changes in genes specifically associated with neuronal communication.[8] Researchers in that study used a cohort of 35,500 samples (12,000 ASD patients) to identify 102 ASD risk genes with 26 demonstrating significant correlations with autosomal dominant neurodevelopmental disorders and another 30 having no previous relationship with ASD.[8] These genetic studies suggest that unique cell types including neurons are different in ASD. Single nucleotide polymorphisms (SNP) are postulated to be the source of most genetic variation in disorders with behavioral phenotypes, but recently it has been found that rare copy number variants (CNV) can also have an influence on phenotype in both behavioral and cognitive disorders. CNV's are known to cause diseases with ASD-like behaviors such as Fragile X syndrome.[9] Gamma-Aminobutyric Acid A receptor Beta3 subunit (GABRβ3) is a protein subunit for ligand gated ion channel Gamma aminobutyric acid ($GABA_A$) that is critical for ion channel function, the inhibition of neurotransmission. Comparative genomic

hybridization tools used to analyze the GABRβ3 gene in the novel maternal 15q duplication model found that CNVs were present that led to methylation differences between parental variants that inhibited gene regulators from binding to the DNA and resulted in gene expression reductions of *GABRβ3.*[10] Current genetic studies in ASD have identified unique SNP's in genes associated with neurotransmission.[11,12] Genotype studies of GABRβ3 using buccal swabs from 530 participants (N=530 with 412 control and 118 ASD patients) found that three different SNPs were found on chromosome 15 in ASD participants.[11] Genetic alterations have been denoted in glutamatergic receptors as well. Glutamatergic receptors, N-Methyl-D-aspartic acid or N-Methyl-D-aspartate, (NMDA), and α-amino-3-hydroxy-5-methyl-4-isoxazolepropionic acid, (AMPA), are responsible for the excitation and depolarization of the post-synaptic neuron transmitting the action potential. Mutations in these cell receptors can cause inactivation that can affect neurotransmission. Genetic analysis of blood from 151 ASD patients showed that four of the twelve unique SNPs in the NMDA glutamate receptor 2B *(GRIN2B)* were associated between haplotypes, a group of genes inherited from one parent.[12] Additionally, knock out studies of CPLX1 (Complexin 1) in mice displayed social behavior deficits that were thought to be related to calcium-mediated receptor exocytosis as the protein regulates fusion of synaptic soluble NSF attachment protein receptor (SNARE) vesicles to regulate glutamate release.[13,14] CPLX1 has also been found to be affected by CNVs that are specific to SNARE vesicle exocytosis in neurons, which could easily affect neural function.[15] The previous studies focus on variations in single genes i.e. *GABRβ3*, *GRIN2B,* and *CPLX1* in ASD; however, fragile X, tuberous sclerosis complex, and chromosome 15 deletions are disorders with unique, single gene etiologies that exhibit ASD behaviors in some but not all of patient base.[16] It is unlikely that a

single gene mutation results in ASD behaviors, but rather a poly-genetic profile is associated with ASD behaviors that contributes to disrupted neuronal function.

Intraneuronal Communication between Pyramidal and Interneurons in the ACC

ASD is a neurodevelopmental disorder with a likely pathophysiological underpinning associated with neuron-to-neuron communication between brain regions that result in social ineptitudes and common overstimulation. The anterior cingulate cortex (ACC) is a brain region that is involved in emotional and attentive responses to stimulation in mammalian species as shown through functional magnetic resonance imaging (fMRI) studies.[17] Activation of the ACC occurs through the excitatory actions of glutamate neurons in the brain via synaptic transmission between two cells termed the presynaptic and postsynaptic cells. The two cells communicate via chemical signals through specific regions of the postsynaptic neuron known as the dendrite. Inhibition of glutamatergic action potentials is attributed to the release of GABA neurotransmitter from GABAergic neurons, or interneurons. Binding of GABA to GABAergic receptors on postsynaptic glutamatergic neurons opens ion channels to hyperpolarize the cell. Neurabin II, or Spinophilin, is a protein that is known to regulate dendritic spine density and synaptic activity, which specifically relates to GABA neurotransmitter release due to the necessity of a mature and functional dendritic spine. Researchers found that Spinophilin knock-out mice had increased dendritic spine number, and a 34.6% increase in spine density.[18] In the same study, cultured neurons from the knock-out (KO) mice demonstrated a larger number of filopodia, plasma membrane protrusions the cell uses to probe its environment, even though the KO mice had the same amount of nerve terminals as the wild-type (WT) mouse strain.[18] Post-synaptic density protein 95 (PSD-95) is another anchoring protein that is involved specifically in the localization of glutamate receptors AMPA and NMDA.[19] *De novo* CNVs studies comparing

ASD, schizophrenia, and attention deficit hyperactivity disorder (ADHD) patient's DNA to their parents revealed that no mutations were found in glutamate receptors but instead mutations were found in glutamate receptor scaffold-associated signaling proteins such as Membrane Associated Guanylate Kinase (MAGUK) scaffold proteins which function in cellular signal transduction and are strictly regulated by phosphorylation.[20,21] Scaffold-associated signaling proteins such as spinophilin and PSD-95 bring synaptic elements close enough to participate in the signaling cascade. Mutations in signaling proteins could cause disruptions in cell survivability, gene transcription, mRNA translation, protein folding, and even dendritic development that could play a role in ASD progression and etiology.[20] Evidence for these disruptions in ASD has not been completely characterized; but, four possible signaling scenarios could exist between excitatory, glutamatergic pyramidal neurons and inhibitory, GABAergic interneurons in the ACC of ASD including (1) pyramidal to pyramidal disruptions, (2) pyramidal to interneuron disruptions, (3) interneuron to pyramidal disruptions, or (4) interneuron to interneuron disruptions.[22] Alterations to one or both cell types may contribute to an excitatory and inhibitory (E/I) imbalance in ASD.

ASD Co-Occurrence with Epilepsy

A link between ASD and GABAergic (inhibitory) dysfunction has been shown through investigations of co-morbid diseases with ASD. Epidemiology studies have found that ASD has a 33% comorbidity with epilepsy affecting one third of the ASD community.[16] In epilepsy, it has been shown that GABAergic inhibition counterbalances glutamatergic excitation to prevent excessive neuronal firing. Drugs that enhance GABAergic conductance i.e., phenobarbital were used in rats to show desynchronize convulsive actions to moderate physiological levels of chloride (Cl^-) ions. Chloride ions are the main negative charge carrier involved in signal conductance and are responsible for hyperpolarizing the cell to inhibit action potentials when

GABAergic ion channels are activated.[23] However, phenobarbital, a drug known to increase the inhibitory actions of GABA, had no effect on convulsions when Cl^- levels were increased until bumetanide was used to lower Cl^- levels back to a moderate physiological level. This phenomenon occurs because when an increased amount of Cl^- is in the cell it results in a decrease in the inhibitory power of GABA neurotransmitter which results in seizures, which also explains why bumetanide is able to restore the inhibitory effects of phenobarbital, by lowering Cl^- levels.[24] Researchers studying the co-occurrence of epilepsy and ASD found the chance that epilepsy occurred in the ASD patient increased as their IQ decreased. This research, done with N=2644 ASD patients, compared co-occurrence rates based on IQ groups (<40, 40-50, 50-70, >70) and found the highest rate to be 46% in the <40 group. These findings suggests that the pathology of ASD intertwines with epilepsy pathology and could be associated with the E/I neuronal imbalance.[16]

Neurotransmitter Serum Levels Support E/I Imbalance

It is hypothesized that enhanced glutamatergic signaling might be present in ASD with support from correlations between plasma levels of glutamate and the severity of autism.[25–27] Modulation of glutamate transporters can occur through either slow or rapid regulation by negative feedback systems and amino acid phosphorylation that facilitates glutamate excitotoxicity in ASD.[28] A study of 931 participants using blood plasma of ASD patients found significant associations between glutamate signaling genes such as GRIN2B and hyperactivity/ impulsivity symptom severity in ASD.[26] A similar study using twenty ASD patients and typically developing (TD) controls showed that ASD patients had a 57% increase in GABA, a 36% increase in glutamate neurotransmitters, and a 13% increase in the glutamate/GABA (E/I) ratio measured via enzyme-linked immunosorbent assay (ELISA).[25] Additionally, plasma studies

using forty ASD and thirty-eight TD age-matched controls indicated that the ASD group demonstrated a significant increase in GABA levels and glutamate/glutamine ratios when ELISA was performed thus implicating a possible impairment in the GABA/glutamate balance that results in increased glutamate neurotransmission in ASD.[27] Glutamate and GABA neurotransmitter metabolism is hypothesized to play a role in cortical excitability. GABA neurotransmitter, formed from glutamate by glutamic acid decarboxylase 65 (GAD65), is "pooled" in nerve terminals at 50-100 mM concentrations; whereas GABA neurotransmitter synthesized by glutamic acid decarboxylase 67 (GAD67) is distributed into the neuronal cytosol. Gad67 KO mice die shortly after birth and have 7% of the brain GABA concentration of WT, but the mice heterozygous for GAD67 have 65% of the brain GABA concentration.[29] Functional GAD proteins are also inhibited by GABA concentration in a negative feedback loop. Studies have suggested that increased GABA levels decrease the activity of GAD and therefore decrease GABA synthesis by 70% in 24 hours.[29] It is also suggested that glutamatergic neurons expressing GABA transporters are able to uptake released GABA neurotransmitter and recycle the molecule to form glutamate.[29] The plasma studies of glutamate compared in parallel with the metabolism of GABA could suggest that there are higher levels of GABA in the blood plasma because of the negative feedback loop that disables GAD activity and because glutamatergic neurons are capable of recycling released GABA into Glutamate.[29]

Brain imaging of live ASD patients is a technique that can be used in living ASD patients to determine changes in unique brain regions that may occur due to possible alterations in neurotransmission. Magnetic resonance imaging (MRI) studies have shown that individuals with ASD have a 5-10% enlargement in total brain volume in young children compared to TD peers as well as a 6-12% increase in gray matter volume in adolescence.[30] This enlargement of grey

matter in ASD could be attributed to abnormal cell proliferation that occurs during the first and second trimesters of pregnancy. Disruption of cellular proliferation can affect differentiation, maturation, and concentration. MRI studies were used to determine that ASD neuronal progenitor cells displayed excessive proliferation when compared to TD neuronal progenitor cells in toddlers. To gain neural progenitor cells for the study, researchers took induced pluripotent stem cells from fibroblasts in living ASD toddlers and differentiated them into neurons which allowed for the study of neuronal maturation and growth regulation.[31] Imaging of brain areas associated with social behaviors are particularly important in ASD studies. The social brain is a term that encompasses many specialized but shared cognitive, emotional, and social brain systems that mediate social interaction.[32] For example, the amygdala is important for recognizing expressions such as fear while the anterior cingulate cortex (ACC) is involved in complex cognitive functions such as empathy and impulse control.[33] fMRI of 1,112 participants (539 ASD, 573 controls) showed that ASD demonstrates reduced functional connectivity between the caudal ACC and sensorimotor sub-regions that are thought to contribute to the severity of ASD.[17] Also, fMRI studies using 21 ASD patients and TD controls implicated differences of the mirror neuron system in the fusiform, temporal, and parietal brain regions thought to contribute to social deficits.[34] Not only have genetic studies supported an imbalance in excitatory and inhibitory neurotransmitters[25], but proton magnetic resonance spectroscopy ([1H]MRS) in the striatum and medial prefrontal cortex of ASD patients demonstrated significant reductions of glutamate in the striatum that was correlated with worsening social function.[35] Overall, brain imaging studies of ASD have one common theme: differences in total brain volume when compared to TD children does correlate with social communication deficits.

BDNF/NTRK2 Signaling Cascades

ASD behaviors could result from synaptic malformations or dysfunction of GABAergic and glutamatergic signaling in the ACC brain region. A current need in ASD research involves studies of dendritic spine development and plasticity in ASD. Dendritic spines as mentioned previously are small protrusions extending from dendrites to serve as the postsynaptic site of excitatory glutamatergic and inhibitory GABAergic synapses in the brain. Brain-Derived Neurotrophic Factor (BDNF) is a growth factor that participates in axonal and dendritic differentiation during embryonic development, neurogenesis, and synaptic maintenance and plasticity.[36,37] BDNF is synthesized in the endoplasmic reticulum as Pro-BDNF, a precursor to the mature form that undergoes cleavage of the terminal domain to become mature-BDNF.[36] BDNF binds to the neurotrophic receptor tyrosine kinase 2 (NTRK2-gene and trkB-protein) to induce three distinct signaling pathways: Ras/ mitogen-activated protein (MAP) kinase, Phospholipase C, and Phosphoinositide-3' (PI3) kinase that are involved in neurite outgrowth, neurogenesis, and synaptic plasticity.[38] The BDNF-NTRK2 pathway can affect the expression of the GABAergic receptor families, $GABA_A$ and $GABA_B$. For example, $GABA_A\alpha$ and $GABR_A\beta$ receptors (multiple subunits) form ligand-gated ion channels, ionotropic channels, while $GABA_B$ receptors (GABBR1 and GABBR2) heterodimerize to form G-protein coupled receptor channels.[39] The GABBR1 subunit contains the GABA binding site but cannot activate the G-protein without dimerization of the GABBR2 subunit that contains a heptahelical domain that allows for a functioning G-protein coupled receptor.[40] The $GABA_B$ G-protein coupled receptor is involved in pumping K^+ out of the cell, bringing Ca^{2+} into the cell and the inhibition of adenylyl cyclase that result in lowering cyclic adenosine monophosphate (cAMP) levels. These functions enhance GABA receptor signaling which increases the inhibitory actions of GABA to regulate glutamatergic signals.[41] For example, GABAα1 are membranous pore forming proteins that

allow chloride to flow into the cell upon GABAergic binding. *GABRA1* gene expression and $GABA_A\alpha$ translation can be activated by the binding of BDNF protein to the trkb receptor. Binding of the GABA neurotransmitter ligand to the $GABA_A\alpha1$ receptor causes a conformational change, dimerization, and trans-autophosphorylation of trkB on conserved tyrosine residues. Effector proteins can dock on trkB tyrosine residues and trigger downstream signaling cascades such as transcription activation. Alterations of trkB signaling is detrimental to synaptic plasticity and survival of neurons. For example, downregulated transcription of $GABA_A\alpha1$ reduces calcium signaling, which we know is necessary for an action potential.[38,42] The $GABA_A\beta$ proteins are also part of a ligand-gated ionic channel family and are regulated in the same manner as $GABA_A\alpha$. After translation, proteins encoded from GABRB receptor genes play an important role in the formation of a functional inhibitory GABAergic synapse in addition to mediating synaptic inhibition through GABA-gated ion channels.[43] Our laboratory has previously demonstrated that gene expression using laser captured microdissected pyramidal neurons for the trkB gene (NTRK2) was significantly lower in ASD anterior cingulate cortical neurons as compared to TD cells.[44] Similar studies have shown the importance of genetic regulation and precise function of the BDNF-NTRK2 signaling cascade for axonal and dendritic growth as well as a functional GABAergic synapse.[45–47] The BDNF signaling cascade of PI3K activates the mammalian target of rapamycin (mTOR) protein that influences protein translation from messenger Ribonucleic Acid (mRNA). The dysregulation of the PI3K-Akt-mTOR pathway can disrupt protein synthesis at neuronal synapses possibly associated with ASD given that mature signaling pathways are responsible for development of the cortex, synaptic function, and synaptic plasticity.[47]

Using a mouse model of *Mecp2,* a gene encoding for a protein that modifies chromatin to regulate gene expression and is highly abundant in the brain, knockdown it was found that dendritic atrophy occurred with *Mecp2* knockdown and could be rescued by an overexpression of *BDNF*.[48,49] Hippocampal neurons infected with an adenovirus vector expressing the inactive trkB isoform was used to demonstrate that presynaptic expression of Tyrosine kinase lacking isoform (T1) inhibited BDNF enhancement of synaptic transmission by the inhibition of specific tyrosine kinase phosphorylation. This study shows that the dimerization and autophosphorylation of the kinase domain in Trk receptors is essential for receptor function, the activation of signaling pathways.[45,46] BDNF is implicated in multiple neurodegenerative disorders due to trkB's ability to regulate expression of genes involved in neural plasticity and cell survival. Taken together these studies highlight the role of BDNF in the connectivity of neuronal networks that is required for synaptic plasticity. BDNF-TrkB signaling is a potential pathway that could be disrupted in excitatory and inhibitory neurons of the ACC in ASD. Additionally, BDNF-immunohistochemistry specifically in frontal cortical neurons was notably increased in TD tissue as compared to ASD tissue.[50] Studying regulation of the GABAergic receptors leads researchers to believe the need for precise and regulated BDNF expression in the cell is necessary to establish connectivity of the neuronal network as dysregulation leads to dysfunctional synapses. These findings suggest BDNF-TrkB deficiencies in both a cell- and region-specific pathology in ASD; thus, providing further support for a need to identify the precise source of the excitatory to inhibitory imbalance in ASD.

Proinflammatory Disturbances Observed in ASD Etiology

Neuroinflammatory mediators are a protective mechanism that could impact GABAergic and glutamatergic signaling. Glial cells are important neuroinflammatory cells in the brain.

Microglia are specialized glial cells that function as macrophages in the CNS and release cytokines that can directly impact organization and function of dendritic spines on glutamatergic and GABAergic neurons.[51] Proinflammatory and immunoinflammatory disturbances observed in the etiology of ASD have led researchers to investigate cytokines. Thirty ASD and age/gender-matched controls used an ELISA assay to show that blood serum levels of visfatin, resistin, and TNF-alpha were significantly higher in ASD children.[52] Our laboratory recently demonstrated altered gene expression levels of anti- and pro-inflammatory signaling molecules in both gray matter (GM) and white matter (WM) tissue in the ACC implicating a possible unique cytokine profile that may be associated ASD.[53] PARP1, (Poly(ADP-ribose) polymerase 1) a protein activated by DNA damage, plays an important role in the regulation of these anti- and pro-inflammatory mediators by controlling gene expression using transcriptional regulation to act as a coactivator/corepressor and to stabilize mRNA of chemokines and cytokines after transcription.[54] Altered expression of neuroinflammatory mediators may be associated with GABAergic changes.

Conclusion of GABA Dysfunction

A growing body of literature supports GABA dysfunction in ASD that may be related to the BDNF-NTRK2 signaling pathway, but little has come from postmortem literature of donors that were diagnosed with ASD. Evidence of the excitatory and inhibitory neuronal imbalance in ASD includes blood plasma levels and fMRI studies that show differences when compared to TD which can be used in the future as both a diagnostic tool and a novel treatment.[55] Polymorphisms in genes *GABRβ3*, *GRIN2B,* and *CPLX1* have been found to be significantly associated with ASD, as well as CNVs providing more evidence for the dysregulation of GABA genes in afflicted patients due to their appearance in disorders such as fragile X and tuberous sclerosis

complex that are highly associated with ASD.[9,10,12,16] In epilepsy, a condition found to co-occur with ASD, drugs enhancing GABAergic action, phenobarbital and bumetanide, were found to reduce seizure effects by counterbalancing glutamatergic excitation and restoring E/I cross-talk.[24] Alterations of the BDNF-TrkB pathway, such as the inability to phosphorylate the TrkB receptor, that may affect GABAergic signaling have been shown in glutamatergic neurons in ASD.[44] Pathology and pathophysiology studies from those directly affected with ASD are vital. The study here will seek to identify distinct synaptic pathology that could be related to the excitatory/inhibitory theory of ASD in the ACC.

Hypothesis

The proposed studies will use postmortem brain tissue from typically developing (TD) age-matched brain donors and donors that were diagnosed with ASD to determine if synaptic pathology related to GABAergic neurotransmission is found in the ACC. Specifically, laser capture microdissection (LCM) will be used to isolate pyramidal neurons in the ACC to determine alterations in gene expression of GABAergic receptors. Immunoblotting will be used to determine changes in synaptic protein expression in the ACC of punch-dissected tissue homogenates. These experiments were created to satisfy the hypothesis that the synaptic pathology associated with GABAergic transmission is found in ASD.

CHAPTER 2. MATERIALS AND METHODS

Brain Tissue

Postmortem human brain tissue from the frontal cortex (BA10) and ACC (BA24) from donors with ASD and age-matched typically developing (TD) control specimens were obtained from Autism BrainNet and NeuroBioBank. Tissues were matched a priori by the brain bank using medical records, clinical information, and postmortem tissue information including age, postmortem interval (PMI), and RNA Integrity Number (RIN) (Table 1).[56] Cause of death for TD control donors included drowning and trauma. The cause of death for ASD donors included: asphyxia, trauma, ketoacidosis, and bowel obstruction. This information has not been added to Table 1 to ensure the identify of donors remains anonymous. ASD specimens have confirmed diagnosis by meeting diagnostic criteria provided by a team of clinicians that used the autism interview and medical records when available to confirm ASD diagnosis. These studies use postmortem human tissue and are not considered human research by the ETSU institutional Review Board.[56]

Table 1. Subject Demographic Information for Donor Tissues Used for Immunoblotting

Pair	ID	Gender	Age	RIN	PMI	Assay	Tissue
Control							
1	AN14757	M	24	7.8	21.3	WB, PCR	BA10, BA24
2	AN07176	M	21	7.6	29.9	WB	BA10, BA24
3	AN07444	M	17	6.1	30.8	WB, PCR	BA10, BA24
4	5408	M	6	5.8	16.0	WB, PCR	BA10, BA24
5	4848	M	16	7.6	15.0	WB, PCR	BA10, BA24
6	5342	M	22	8.1	14.0	WB, PCR	BA10, BA24
7	5079	M	33	7.3	16.0	WB	BA10, BA24
8	m3231m	M	37	7.4	24.0	WB, PCR	BA10, BA24
9	4590	M	20	6.8	32.9	WB	BA10, BA24
11	1105	M	16	7.8	28.9	WB	BA10, BA24
12	12137	M	31	7.3	26.2	WB	BA10, BA24
14	4670	M	4	6.2	17.0	WB, PCR	BA10, BA24
Mean			20.583	7.15	22.66		
SEM			2.87	0.22	2.01		
ASD							
1	AN04166	M	24	8.1	18.5	WB, PCR	BA10, BA24
2	AN03935	M	19	7.0	28.1	WB	BA10, BA24
3	AN02987	M	15	6.7	30.8	WB, PCR	BA10, BA24
4	5144	M	7	8.0	3.0	WB, PCR	BA10, BA24
5	5302	M	16	6.6	20.0	WB, PCR	BA10, BA24

6	5176	M	22	7.1	18.0	WB, PCR	BA10, BA24
7	5297	M	33	7.1	50.0	WB	BA10, BA24
8	5027	M	37	7.7	26.0	WB, PCR	BA10, BA24
9	4999	M	20	7.0	16.1	WB	BA10, BA24
11	5403	M	16	6.6	23.7	WB	BA10, BA24
12	11989	M	30	7.7	23.2	WB	BA10, BA24
14	5308	M	4	7.0	21.0	WB, PCR	BA10, BA24
Mean			20.250	7.2	23.2		
SEM			2.83	0.15	3.18		

RIN, RNA integrity number

WB, Western Blotting

Tissue Preparation and Sectioning

Frozen tissue blocks of BA24 and BA10 were sectioned using a cryostat microtome (Leica CM3050S) at -20ºC. Tissue blocks were left to thaw inside the Leica for one hour prior to sectioning and Optimal Cutting Temperature compound (Sakura, Tissue-Tek O.C.T. Compound, cat# 62550-01) was used to adhere the tissue to the mounting block. Section thickness varied including 10 µM for laser capture microdissection experiments and 40 µM sections for punch dissection homogenates. Laser capture microdissection, 10 µM, sections were placed on superfrost plus microscope glass slides (Fisherbrand, cat# 12-550-15), labeled, and stored in microslide black boxes at -81ºC. Additionally, brain tissue was punch-dissected, 40 µM thickness, using a 3.5 mm trephine. Tissue punches were placed in 1.5 mL Eppendorf tubes and stored at -81ºC until use. Tissue pairs of ASD and TD were prepared and stored together to

ensure identical handling. The central point of the tool was placed over layer three of the neocortex in both BA10 and BA24 when punch-dissecting.

Laser Capture Microdissection

Ten-micron thick sections were used for Laser Capture Microdissection (LCM). Cells were identified using a Cresyl violet stain from the Applied Biosystems (Thermo Fisher Scientific, Arcturus™ HistoGene™ Staining Solution, Cat# 00728573). In brief, frozen human postmortem brain tissue sections were fixed, rehydrated, incubated with Cresyl violet for 45 seconds, and dehydrated with 75% EtOH, 95% EtOH, and 100% EtOH for 30 seconds each, and left in Xylene for 5 minutes. Once the tissue was dry, the section is desiccated for proper transport to the laser capture microdissection instrument which uses infrared laser technology to capture the neuronal soma. LCM was performed using an ArcturusXT instrument (Life Technologies AXT 2142) to visualize and capture pyramidal neurons (Figure 1A) from the ACC or BA24 at 60X magnification. The Arcturus XT software tracks the number of cells during a single capture, but the captured cell type and neocortical layer is dependent upon morphological identification and neuronal size measured by the user. Pyramidal neurons are triangular in shape and get larger as neocortical layer gets deeper, which is visible on tissue by observing neuron density. Pyramidal neurons in neocortical layer 2 are approximately 15-20 μm in width. Neurons with other cell bodies, astrocytes or glia, nearby were not chosen to reduce other neuronal mRNA from capture. Infrared (IR) laser technology is used to capture approximately six hundred neurons onto CapSure macrocaps (Life Technologies, Arcturus™ CapSure HS LCM Starter Pack, cat# 10284-05). The tissue is manually inspected at a higher power to ensure that the cell has been lifted onto the cap (Figure 1B). Lastly, the cap can be visualized at 20X magnification in the QC station and the number of cells counted to compare against actual

number of cells identified by the Arcturus and lifted from tissue (Figure 1C). After the capture is complete, the cap is visualized under a dissecting microscope to remove any excess tissue attached by scraping it off with a syringe needle. The cap, now with only selected neuronal cells attached, is placed in a 0.5 mL tube containing 55 µL of extraction buffer solution (Thermo Fisher, Arcturus™ PicoPure™ RNA Isolation Kit, cat# 00809988) and incubated in a 42^{o}C water bath for 30 minutes. Cells are then removed from the water bath, the extraction buffer is centrifuged to the bottom, and the Eppendorf tube is stored at -20^{o}C until used to extract purified RNA.

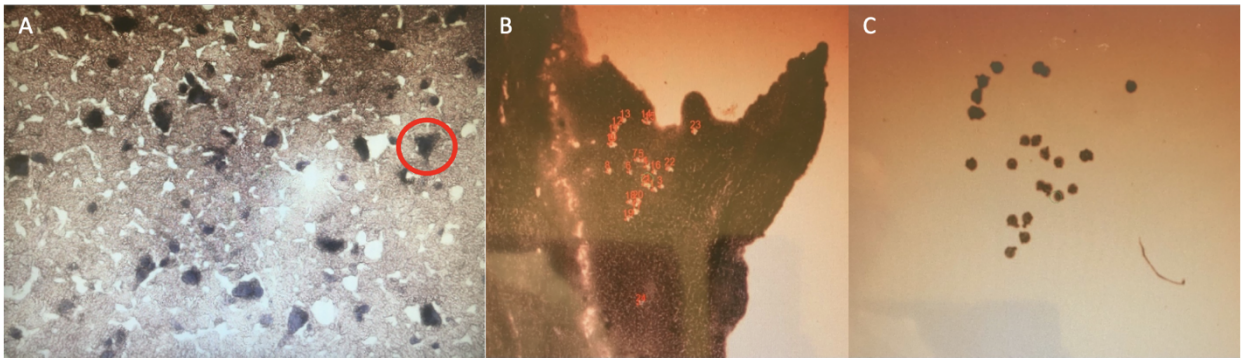

Figure 1. Images from ArcturusXT of human BA24 tissue. A) Pyramidal neuron, circled in red, are imaged from the ArcturusXT instrument at 60X magnification in the ACC of postmortem human brain tissue in Neocortical layer 2. B) ACC tissue post cell soma capture. C) Captured pyramidal cells visualized on CapSure Macrocap to ensure complete capture.

RNA Purification

RNA extraction from laser captured cells was performed with the Arcturus™ Picopure™ RNA Isolation Kit (cat# KIT0204, Thermofisher, Waltham, MA) with a column-based binding and on-column DNase treatment. Columns from the kit were first conditioned with 250 µl of conditioning buffer (CB) at room temperature for 5 minutes. The columns were then centrifuged at 16,000g for 1 minute and the flow-through, CB, was discarded. 55 µl of 70% EtOH, equal to the amount of extraction buffer, was added to the column along with the extraction buffer and the mixture is centrifuged at 100g for 2 minutes followed by 16,000g for 30 seconds. For maximum binding, the flow-through can be placed back inside the column and the centrifugation repeated. After RNA is bound to the column beads, 100 µl of wash buffer 1 (W1) is added and centrifuged at 8,000g for 1 minute. The on-column DNase treatment was prepared in a separate tube with reagents as follows: 5 µl DNase 1 and 35 µl Buffer RDD, both from the Qiagen RNase-Free DNase Set (Qiagen, cat# 79254). DNase treatment was gently mixed by inversion of the Eppendorf tube and 40 µl was pipetted on top of the column beads and left to incubate for 15 minutes at room temperature. 40 µl of W1 was added to the column at the end of 15 minutes and centrifuged at 8,000 x g for 15 seconds. For thorough washing, 100 µl of wash buffer 2 (W2) was

added to the column and centrifuged at 8,000 x g for 1 minute and then repeated with fresh W2 and centrifuged at 1,000 x g for 1 minute and 16,000 x g for 1 minute. After the final centrifugation at 16,000 x g twice for 2 minutes. At this time, the column is placed into a fresh 0.5 ml Eppendorf tube where 16 µl of elution buffer is added and let incubate for 5 minutes at room temperature. This is centrifuged, this sample can be reverse transcribed into cDNA. Forty micron (40 µm) thick sections are used for punch dissected positive control samples. To purify RNA from punch tissue, 200 µl of extraction buffer and 200 µl of 70% EtOH are added while the Eppendorf tube containing the tissue is still in the -80˚C freezer. The tubes can then be removed, placed on ice, and vortexed to ensure the tissue has dissolved into the liquid mixture. The same protocol as above is used to purify RNA except 18 µl of elution buffer is used instead of 16 µl.

cDNA Synthesis

RNA samples were reverse transcribed into cDNA using the Superscript III kit (Life Technologies, First-Strand Synthesis SuperMix for qRT-PCR, cat# 11752-050) using oligodTs and random hexamer primers. Each cDNA sample contains a mixture of 10 µl 2x RT Reaction Mix, 2 µl RT enzyme mix, and 8 µl purified RNA. This mixture is run on a Bio-Rad Thermocycler (Bio-Rad, T100™ Thermal Cycler, 1861096) for 10 minutes at 25˚C, 30 minutes at 50˚C, and 5 minutes at 85˚C. At step four the thermocycler pauses and 1 µl RNase H is added to the sample followed by a 20-minute incubation at 37˚C at which time the cDNA is complete and can be stored at -20˚C until analysis (Appendix Table 1).

Primer Creation

Primers annealing to GABAergic receptor genes expressed in the LCM pyramidal neurons were created by using NCBI Gene to obtain all variants for a specific gene in *Homo sapiens.* All variants were compiled into a word document and the shortest variant was used to

create the primers and then checked with NCBI blast to ensure the spanned exons were present in each gene variant. A folding assay was performed with chosen sequences using the mFold webserver, free on the list serve by The RNA Institute College of Arts and Sciences University of Albany, to identify folding patters for mRNA sequences at 61˚C and 65˚C. Ionic conditions for Magnesium and Sodium were changed to 2 mM and 50 mM respectively. Both sequences were analyzed for secondary structure formation at the two temperatures. Next, the sequence was removed of any sequence identifiers using the Bio-Web sequence cleaner. The sequence was then loaded into the Integrated DNA Technologies (IDT) PrimerQuest software to identify potential 100 bp sequences. Next, potential primer sequences were analyzed for gene similarity to other genes in the human genome. If the sequence was 66% or more that potential primer was disregarded. Amplicon size was set to 90-120 base pairs and the primers selected spanned at least one exon junction to ensure mRNA binding. Two primers were ordered for every gene, when possible, but only the best primer was used for gene expression studies (Appendix Table 2). In some cases, the primer was not made through IDT and was instead ordered directly from Qiagen using their proprietary Quantitect software as noted in Appendix Table 2.

PCR Amplification

Primers were optimized for annealing temperature and primer concentration using punch dissected sample, BA24, for enzymes used in downstream assays. The annealing temperature is the temperature at which the enzyme and primer work best together to amplify cDNA strands. Typically, the annealing temperature is 5°C below the primers melting temperature and this was visualized with The Agilent Tape Station 2200 (Agilent Technologies C295A) using at least 5 temperatures that ranged from 52º to 65º Celsius. Primer concentration was optimized at the optimal temperature. Primer concentration is important to optimize to conserve reagents as well

as to confirm only one amplicon is amplifying. Complete optimization details, temperature, and primer concentration are outlined in Appendix Table 3.

Primers were also optimized for laser captured parameters of cycle. A nested PCR method was used to amplify cell captures so that the Stratagene quantitative PCR thermocycler could detect amplification. Pre-amplification cycles were chosen by determining which cycle number gave a reliable threshold count using forty cycles for quantitative-RealTime-PCR (q-RT-PCR) run. The mRNA captured from 500 Pyramidal neurons in BA24 of tissue donors that had been converted to complimentary DNA (cDNA) was diluted 6 µl H2O: 2 µl cDNA to conserve tissue. Pre-amplification reactions included 2X master mix enzyme with dNTPs and magnesium (Appendix Table 4), water, and gene specific primer (10X) in a volume of 11.5 µl. Template cDNA from each donor (approximately 600 cells) was added at a constant volume of 0.5 µl of LCM cell cDNA to each reaction. Duplicate reactions were performed for each sample. Pre-amplification thermocycler parameters were optimized for each gene specific primer with a taq-based enzyme (Appendix Table 3). The pre-amplified reactions were used in combination with q-RT-PCR reactions to analyze target genes (GABRA1, GABRA4, GABBR1) in ASD and TD brain donor laser capture samples. Gene selection rationale is outlined in Appendix Table 5. The quantitative PCR reaction mix included water, 10X gene specific primer, and 2X Power-up syber-based enzyme (Appendix Table 4) in a volume of 17 µl; afterwhich, 1µl of each pre-amplification reaction is added to reaction mix. Each pre-amplification target was performed in duplicate resulting in four QPCR reactions for each sample. Two positive control reactions of 1 µl punch cDNA and two blank wells with 1 µl of water were included for each gene. Reaction parameters were optimized using PowerUp enzyme at 40 cycles on an Agilent Stratagene Mx3000 (Agilent Technologies, Stratagene serial#DE10900784). Each target gene was

normalized to two housekeeping genes (18S ribosomal RNA and Beta-2-Microglobulin) during gene analysis.

Immunoblotting

Brain tissue was homogenized with ten seconds of sonication using Tris-EDTA buffer supplemented with protease inhibitors. Protein assays were performed with tissue homogenates using the Micro BCA™ Protein Assay kit (ThermoScientific, cat# SI252807). Bovine serum albumin (BSA) standards were diluted in phosphate buffer saline (PBS) ranging from 200 µg to 2 µg. Dilutions of samples (100-fold and 25-fold) were created using PBS to insure the same refractory index as dilution of standards. Assay with BSA standards and tissue homogenate was incubated at 57°C for one hour and then read using a plate reader at 562 nm wavelength for index determination. Protein homogenate was mixed at a 1:4 dilution with Laemmli/Beta-MercaptoEthanol (βME) loading buffer and heated at 95^{o}C for 5 minutes to be stored at -80^{o}C until use. From the protein assay, the protein homogenates were standardized to twelve micrograms of protein and diluted to make 40 µl total concentration. For each gel, 10 µL of a Precision Protein standard ladder (Bio-Rad, Protein™ Dual Color Standards, cat# 161-0374) was added to demonstrate the molecular weight in kilodaltons. Eleven matched ASD/TD pairs, the protein homogenates, were loaded as singlets on two different 10% SDS-polyacrylamide gels (BioRad, Mini PROTEAN TGX Gels, cat# 456-1084), and 3 wells containing 25 µg, 12.5 µg, and 6.25 µg of protein were loaded for use as a standard. Gels were subjected to electrophoresis for one hour at 100V. Denatured proteins captured in the gel were then transferred onto a nitrocellulose membrane (BioRad, Nitrocellulose Membranes 0.45 µm, cat# 1620115). The nitrocellulose membrane is thoroughly washed and is stained with Ponceau S (SIGMA-ALDRICH, 0.1% Ponceau S, 5% acetic acid, cat #SLCB3855) for later use as a standard and to

confirm successful protein transfer. Ponceau S is removed using 1X PBS-Tween20 (TBST). Following Ponceau-S stain, the nitrocellulose membrane is blocked in 5% skim milk solution for one hour. Protein bound to the membrane are probed with primary antibodies at different concentrations: Spinophilin (1:1,000), PSD95 (1:1,000), IGF1R (1:1,000), mTOR (1:1,000), Aggrecan (1:1,000), PARP1 (1:1,000), CPLX1 (1:1,000), and GapDH (1:10,000) (Table 2 and Appendix Table 6) overnight at 4^{o}C with rotation. Post incubation, membranes were washed three times with 1X PBS-Tween20 for ten minutes and followed with a secondary antibody incubation with either anti-mouse (1:10,000) or anti-rabbit (1:5,000) horseradish peroxidase (HRP)-conjugated secondary antibody (GE Healthcare, ELC™ Anti-Mouse IgG, HRP linked whole antibody, cat#4950492) (GE Healthcare, ELC™ Anti-Rabbit IgG, HRP linked whole antibody, cat# 17065614) at room temperature. Lumagen ECL ultra substrate (Lumagen,Inc, Lumagen ECL Ultra Solution A and B, cat# TMA-100) is used at a 1:10 dilution for each part for visualization using the BioRad ChemiDoc machine (BioRad, ChemiDoc™ Imaging System). Images are obtained using the BioRad ChemiDoc and analyzed by the BioRad ImageLab software to quantify protein band concentration. Next, bound antibodies were removed from membranes using a mild stripping buffer, pH 2.2, for 12 minutes (Abcam). After stripping, the membrane was thoroughly washed, blocked using 5% milk for one hour and re-probed with a different primary antibody overnight (Appendix Table 7). The order of antibody incubation is as such: Day 1 Spinophilin & CPLX1, Day 2 IGF1R & mTOR, Day 3 PSD95, Day 4 PARP1, Day 5 Aggrecan, Day 6 GapDH. Some Antibodies were able to run together because of the molecular size (in kilodalton) of their target and incubation solutions outlined in Table 2 and Appendix Table 7. All buffers used for immunoblotting are found in Appendix Table 8. For protein band analysis, means and standard deviations were calculated for all band densities including

Spinophilin, CPLX1, mTOR, IGF1R, PSD95, PARP1, and Aggrecan for immunoblotting data. Ratios were calculated for each target protein using a housekeeping protein (GAPDH).

Table 2. Proteins Analyzed for Immunoblotting

Protein	Job in VIVO	Kilodalton
Spinophilin	Modulate glutamatergic synaptic transmission & dendritic morphology	130 kDa
PSD-95	Postsynaptic scaffolding protein: clusters glutamate receptors and organizes signaling complexes	95 kDa
IGF1R	Receptor for Insulin-like Growth Factor 1. Regulates cell growth and proliferation	90 kDa
mTOR	Cell survival and dendritic plasticity	289 kDa
Aggrecan	Organization of extracellular nets between neurons	150 kDa
PARP1	Regulator of NF-κB by promoting nuclear translocation	113 kDa
CPLX1	Prevent SNAREs from releasing neurotransmitters until an action potential arrives at the synapse	18 kDa
GapDH	Glycolytic enzyme that catalyzes the conversion of glyceraldehyde 3-phosphate to 1,3-diphosphoglycerate	37 kDa

Statistical Analysis

All data was subjected to tests for normality. Additionally, all data was examined for outliers using both a Grubb's test and a ROUT test. Analysis for differences in threshold cycle used the Livak and Schmittigen method for delta delta Ct values.[57] If data was found to be normally distributed, an unpaired two-tailed Student's *t*-test was used to compare data between ASD and TD donors for immunoblotting data. If data failed tests for normality, a Mann-Whitney test was used to assess statistical analysis between groups. All correlations were performed with

the linear correlation analysis producing a Pearson R-value including those between target expression values and age, PMI, and RIN. Any significant correlation that was found was subjected to a univariate analysis between the groups with the variable used as a confound. Lastly, paired testing was conducted to validate previous statistical methods and shown in the appendix. All data analyses were performed using Graphpad Prism version 9. Statistical significance was determined as a p-value less than 0.05.

CHAPTER 3. RESULTS

Touchdown Assay used for Laser Capture Studies

Touchdown PCR assays were preformed to pre-amplify the desired amplicon for QPCR analysis of GABAergic receptors. This type of assay is novel in the literature for laser capture studies. Extraction of mRNA from laser capture microdissected pyramidal cells (500 cells) in BA24 yields small quantities of cDNA. Touchdown assays for varying cycles (Table 3) and concentration gradients (Table 4) were performed for every gene (GABRA1 shown) that the small amounts were capable of demonstrating reliable threshold scores, the cycle at which linear amplification of cDNA is detected by the Agilent machine, during q-RT-PCR amplification. Representative graphs are shown to demonstrate that genes did exhibit a linear correlation between cycle threshold with preamplification threshold (Figure 2 A) and concentration (Figure 2 B). GABRA4 and GABBR1 threshold tables and graphs are outlined in Appendix Tables 9-12 and Figures 1-2.

Table 3. Cycle Optimization for GABRA1 with HotStar Enzyme

65°C, 58° C w/ HotStar	**2/17/2021**
GABRA1	**Threshold**
19	28.32
22	17.42
25	15.61
Punch	9.0
Blank	36.74
+ Control	23.86

Table 4. cDNA Template concentration check for Threshold

65° C, 58° C w/ HotStar	3/17/2021
GABRA1	Threshold
Full	28.49
Half (1:2)	31.71
Fourth (1:4)	39.64
Punch	16.8
Blank	0
+ Control	25.39

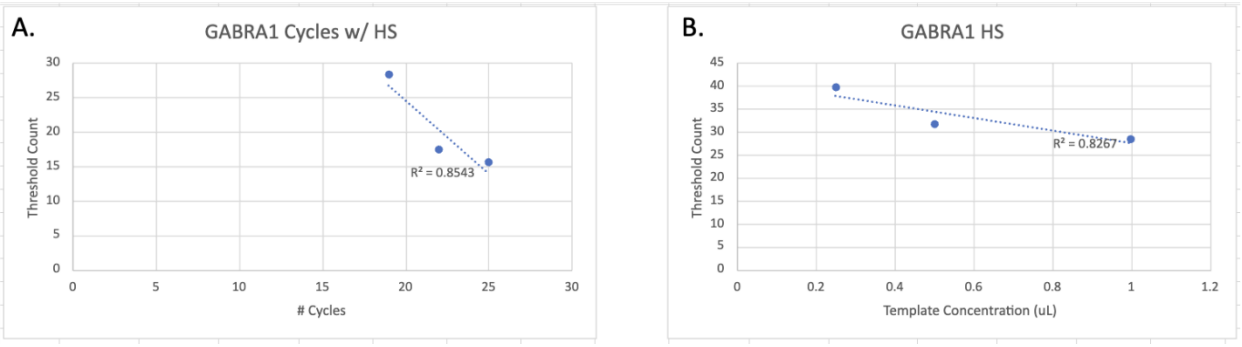

Figure 2. Graphs correlating with cycle optimization and template concentration tables. Panel A denotes the preamplification cycle used for expression of GABRA1. The y-axis is the threshold cycle at which the product approached linear amplification. The x-axis is the number of cycles the cDNA template was pre-amplified using standard PCR. Panel B denotes template concentration to assure cDNA would reach threshold. The y-axis is the threshold cycle at which the product approached linear amplification. The x-axis is the initial cDNA template that was used at no dilution (1), 1:2 dilution and 1:4 dilution.

Gene Expression Differences in ASD Pyramidal Cells

GraphPad Prism version 9 software was used to analyze QPCR data obtained from Agilent Stratagene Mx3000. GABAergic receptor genes including GABRA1, GABRA4, and

GABBR1 were amplified in BA24 pyramidal neurons. Analysis for differences in threshold cycle used the Livak and Schmittigen method for delta delta Ct values. Genes were analyzed by an unpaired Student's *t*-test using ASD and TD brain donors. It was found that no significant differences in gene expression of any of the GABAergic receptors in BA24 pyramidal neurons were present when comparing ASD and TD brain donors (Figure 3 Panel A-C). However, it should be noted that increased expression trends in GABRA4 (Figure 3B) and GABBR1 (Figure 3C) expression are apparent in ASD when compared to TD brain donors.

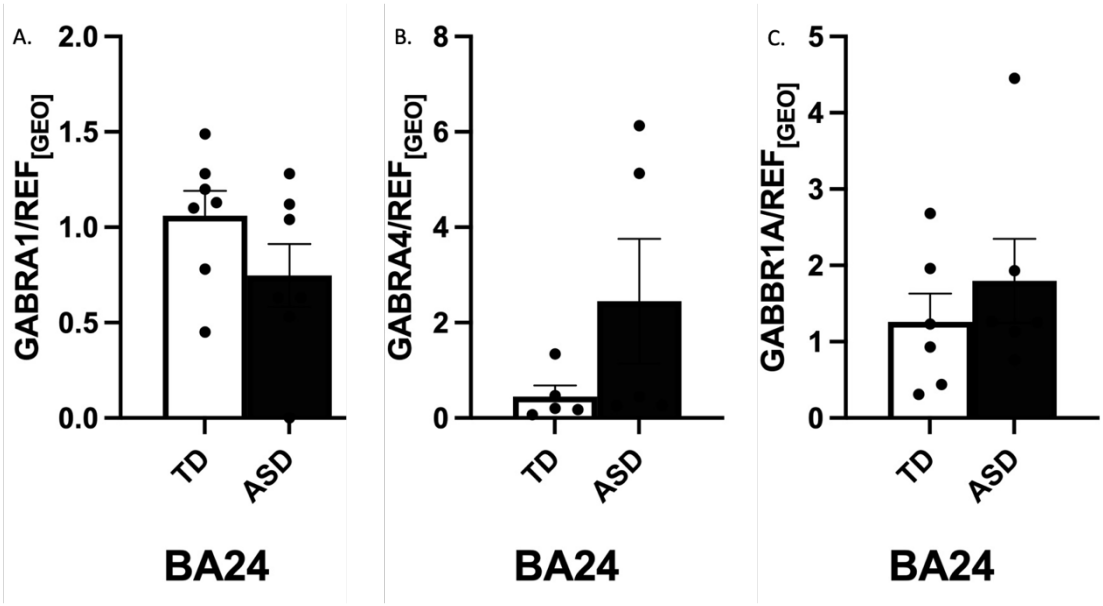

Figure 3. Unpaired analysis of q-RT-PCR data Panel A) Gene Expression of GABRA1 was determined in human postmortem tissue from anterior cingulate, BA24 (N=7) laser capture microdissected brain tissue from TD control tissue (white bars) and ASD tissue (black bars) using the Livak/Schmittagen delta delta Ct method for QPCR. GABRA1 gene expression was normalized to the gene expression of 18S ribosomal RNA and beta-2-microglobulin. An unpaired Student's *t*-test was used to determine statistical significance with $p<0.05$. Panel B) GABRA4 (N=5) and Panel C) GABBR1 (N=6) analysis were performed using the same parameters.

Immunoblotting in the ACC

GraphPad Prism 8 software was used to analyze immunoblotting data obtained from ChemiDoc ImageLab software. Student's unpaired *t*-tests determined that no significant differences in synaptic protein expression for Spinophilin, CPLX1, mTOR, IGF1R, PSD95, or PARP1 were found in gray matter from BA24 (anterior cingulate cortex) or BA10 (frontal cortex) between ASD and TD brain tissue homogenates (Figure 4). While some proteins gave very small concentration differences between the donors, BA10: CPLX1, PSD-95 (Appendix Figure 3 B, E) BA24: Spinophilin, PSD-95, and PARP1 (Appendix Figure 4 A, E, F),

others seemed to have no correlation trends at all and concentrations varied drastically between matched donors, BA10: IGF1R and PARP1 (Appendix Figure 3 D and F) BA24: CPLX1 and IGF1R (Appendix Figure 4 B and D). One noticeable correlation occurs in BA10 Spinophilin which shows a downward trend in ASD (Figure 4A).

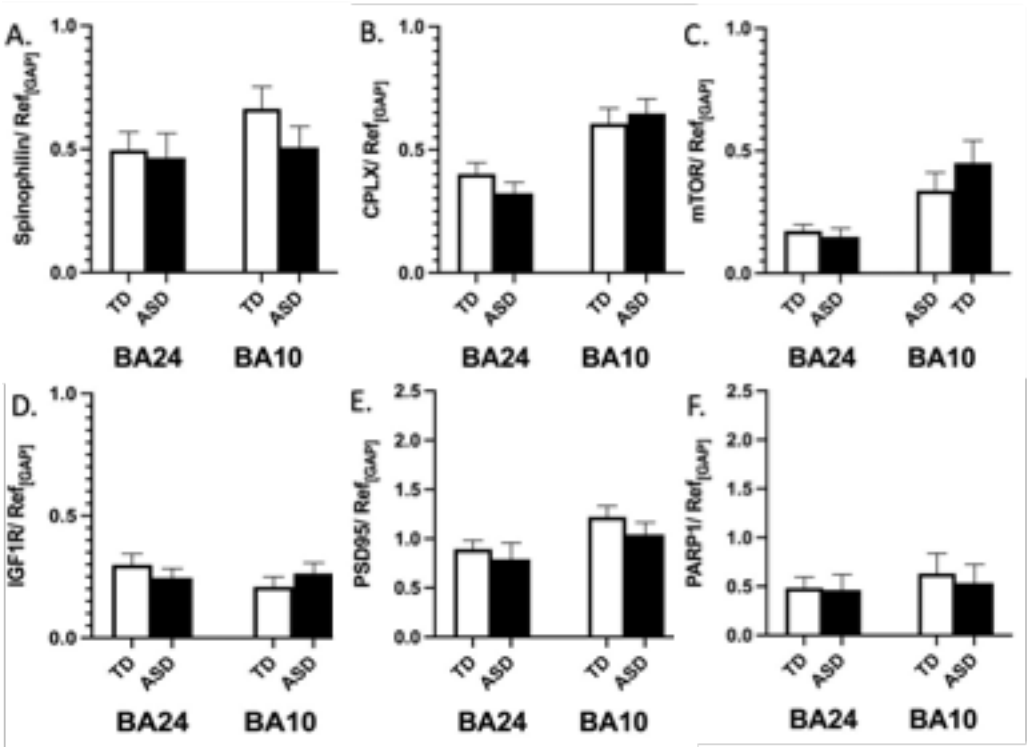

Figure 4. Unpaired analysis of Immunoblotting data. Panel A) Protein Expression of Spinophilin was determined by immunoblotting in human postmortem tissue from frontal cortex, BA10 (N=11), and anterior cingulate, BA24 (N=11) punch-dissected brain tissue from TD control tissue (gray bars) and ASD tissue (black bars). Spinophilin protein expression was normalized to the protein expression of GAPDH. An unpaired Student's *t*-test was used to determine statistical significance of $p<0.05$. Panel B) CPLX1, Panel C) mTOR, Panel D) IGF1R, Panel E) PSD95, and Panel F) PARP1.

Correlations of Demographic Information

The brain tissues that are used in this study are matched by age, RIN and PMI a-priori by the tissue brain banks. The potential effects were examined by using correlations to compare protein and gene expressions to matching factors in the groups. Age was not significantly different between the ASD and TD group (Mean: 20.58, 20.25 SEM: 2.87, 2.83). Significant correlations between protein expression levels for spinophilin, mTOR, IGR1R, PSD 95 and PARP1 with age were noted in the anterior cingulate or BA24 (Table 5). Interestingly, none of

the protein expressions demonstrated significant correlations with age in control donors from the frontal cortex or BA10 only in the combined donor groups for IGF1R and PARP1 (Table 6). Neither RIN (Mean, SEM) nor PMI (Mean, SEM) demonstrated differences between ASD and TD donor groups (Table 1). Although RIN is an important factor in molecular studies, it can be used as a global factor of tissue quality. RIN values did correlate with spinophilin, mTOR, PSD95, and PARP1 in control donor tissue (Table 5). There were no correlations between PMI with any protein expression level in any group (Table 5-6). Additionally, no gene expression levels of any of the GABAergic receptors correlated with age, RIN or PMI (Table 7). Univariate analysis was performed for any protein that demonstrated a significant correlation with a matching factor. No effects of the factor were found for any protein between ASD and TD donor tissues (Table 8). For completeness, a Student's paired *t*-tests were used to determine no significant differences could be found for Spinophilin, CPLX1, mTOR, IGF1R, or PSD95 in grey matter from BA10 or BA24 in the same eleven ASD-TD pairs (Appendix Figure 2-3).

Table 5. Pearson Correlations for Western Blotting Protein Expression Levels vs Potentially Confounding Variables in BA24. *p≤.05, **p≤.01

All donors combined		SPIN	CPLX	mTOR	IGF1R	PSD95	PARP1
Age	Pearson r	-.6121	-.6453	-.4646	.6916	-.5154	-.7105
	Sig. (2-tailed)	.003**	.0012**	.0294*	.0007**	.0141*	.0002**
	N	22	22	22	20	22	22
RIN	Pearson r	-.2720	-.3365	-.0601	.3744	-.2157	-.2808
	Sig. (2-tailed)	.2208	.1257	.7904	.1039	.3349	.2056
	N	22	22	22	20	22	22
PMI	Pearson r	-.0104	-.2909	-.4272	-.1125	-.1537	-.4089
	Sig. (2-tailed)	.9633	.1890	.0474*	.6367	.4946	.0588
	N	22	22	22	20	22	22

Control donors		**SPIN**	**CPLX**	**mTOR**	**IGF1R**	**PSD95**	**PARP1**
Age	Pearson r	-.7945	-.5263	-.6691	.7922	-.6039	-.8478
	Sig. (2-tailed)	.004**	.0963	.0244*	.006**	.0491*	.001**
	N	11	11	11	10	11	11
RIN	Pearson r	-.6795	-.4586	-.6101	.4403	-.6752	-.7982
	Sig. (2-tailed)	.0215*	.1559	.0462*	.2028	.0226*	.0032**
	N	11	11	11	10	11	11
PMI	Pearson r	.2597	.2871	-.2635	-.3226	.4293	.1554
	Sig. (2-tailed)	.4407	.3920	.4337	.3633	.1876	.6483
	N	11	11	11	10	11	11

ASD donors		**SPIN**	**CPLX**	**mTOR**	**IGF1R**	**PSD95**	**PARP1**
Age	Pearson r	-.4935	-.8302	-.3316	.6260	-5138	-.6323
	Sig. (2-tailed)	.1229	.0016**	.3192	.0528	.106	.0368*
	N	11	11	11	10	11	11
RIN	Pearson r	.1394	-.1695	.5434	.2950	.1012	.2236
	Sig. (2-tailed)	.6827	.6184	.0840	.4080	.7672	.5087
	N	11	11	11	10	11	11
PMI	Pearson r	-.1306	-.6854	-.5018	.0703	-.3428	-.6584
	Sig. (2-tailed)	.7019	.0199*	.1158	.8470	.3021	.0276*
	N	11	11	11	10	11	11

Table 6. Pearson Correlations for Western Blotting Protein Expression Levels vs Potentially Confounding Variables in BA10. *p≤.05, **p≤.01

All donors combined		SPIN	CPLX	mTOR	IGF1R	PSD95	PARP1
Age	Pearson r	.3171	.2381	-.3619	.4674	.2786	-.4547
	Sig. (2-tailed)	.1311	.2859	.0823	.0213*	.2343	.0335*
	N	24	22	24	24	20	22
RIN	Pearson r	.2125	.1507	-.3687	.3012	.0589	-.2827
	Sig. (2-tailed)	.3189	.5032	.0763	.1526	.8049	.2025
	N	24	22	24	24	20	22
PMI	Pearson r	-.1906	-.0005	.1850	-.0868	-.3052	-.0482
	Sig. (2-tailed)	.3724	.9963	.3868	.6865	.1907	.8313
	N	24	22	24	24	20	22

Control donors		**SPIN**	**CPLX**	**mTOR**	**IGF1R**	**PSD95**	**PARP1**
Age	Pearson r	.2877	-.0126	-.4918	.5401	.3255	-.5107
	Sig. (2-tailed)	.3645	.9706	.1043	.0698	.3588	.1084
	N	12	12	12	12	10	12
RIN	Pearson r	.1164	-.1046	-.4051	.3968	-.0558	-.3186
	Sig. (2-tailed)	.7186	.7595	.1915	.2015	.8783	.3397
	N	12	11	12	12	10	11
PMI	Pearson r	-.4498	-.2417	.1714	-.5734	.0386	-.3895
	Sig. (2-tailed)	.1423	.4740	.5884	.0513	.9156	.2364
	N	12	11	12	12	10	11

ASD donors		**SPIN**	**CPLX**	**mTOR**	**IGF1R**	**PSD95**	**PARP1**
Age	Pearson r	.3622	.5084	-.2277	.4226	.2461	-.4025
	Sig. (2-tailed)	.2473	.1103	.4767	.1711	.4931	.2197
	N	12	11	12	12	10	11
RIN	Pearson r	.4183	.5444	-.2987	.1786	.1624	-.2632
	Sig. (2-tailed)	.1760	.0834	.3457	.5786	.6539	.4342
	N	12	11	12	12	10	11
PMI	Pearson r	-.0268	-.2085	.2314	.1868	-.4440	-.2076
	Sig. (2-tailed)	.9339	.5383	.4692	.5611	.1986	.5401
	N	12	11	12	12	10	11

Table 7. Pearson Correlations for LCM Gene Expression Levels vs Potentially Confounding Variables in BA24. *p≤.05, **p≤.01

All donors combined		**GABRA1**	**GABRA4A**	**GABBR1**
Age	Pearson r	.1046	.1311	.0353
	Sig. (2-tailed)	.7221	.7181	.9132
	N	14	10	12
RIN	Pearson r	-.09988	-.1627	.2591
	Sig. (2-tailed)	.7341	.6533	.4162
	N	14	10	12
PMI	Pearson r	.0911	.0503	-.2937
	Sig. (2-tailed)	.7565	.8902	.3542
	N	14	10	12

Control		**GABRA1**	**GABRA4A**	**GABBR1**
Age	Pearson r	.1746	-.2493	.1732
	Sig. (2-tailed)	.7081	.6858	.7428
	N	7	5	6
RIN	Pearson r	-.4440	.08075	.6783
	Sig. (2-tailed)	.3183	.8973	.1386
	N	7	5	6
PMI	Pearson r	.4544	-.3608	-.2184
	Sig. (2-tailed)	.3057	.5508	.6776
	N	7	5	6

ASD		**GABRA1**	**GABRA4A**	**GABBR1**
Age	Pearson r	.0617	.2665	-.0524
	Sig. (2-tailed)	.8954	.6647	.9214
	N	7	5	6
RIN	Pearson r	.4898	-.2064	-.1860
	Sig. (2-tailed)	.2645	.7391	.7242
	N	7	5	6
PMI	Pearson r	-.1021	.0494	-.3233
	Sig. (2-tailed)	.8276	.9370	.5319
	N	7	5	6

Table 8. Univariate Analysis with Potentially Confounding Variables for Western Blotting in BA24 that Demonstrated a Significant Correlation in Control Groups. *p≤.05, **p≤.01. ≤.05, **p≤.01.

Variable		**SPIN**	**CPLX**	**mTOR**	**IGF1R**	**PSD95**	**PARP1**
Age	Between group	.724	.109	.521	.126	.513	.837
	Levene's Test	.034	.373	.383	.878	.838	.064
	N	11	11	11	10	11	11
RIN	Between Group	.829		.806		.608	.945
	Levene's test	.078		.200		.049	.098
	N	11	11	11	10	11	11

Table 9. Univariate Analysis with Potentially Confounding Variables for Western Blotting in BA10 that Demonstrated a Significant Correlation in Control Groups. *p≤.05, **p≤.01.

Variable		**SPIN**	**CPLX**	**mTOR**	**IGF1R**	**PSD95**	**PARP1**
Age	Between groups				.306		.665
	Levene's test				.799		.763
	N	12	12	12	12	10	12

CHAPTER 4. DISCUSSION

This is the first study to use laser captured pyramidal neurons from human cingulate cortex in ASD to examine unique cell-specific GABAergic receptor expression. In this study, q-RT-PCR nested amplification was used to quantify gene expression of three different GABAergic receptors (GABRA1, GABRA4, and GABBR1). Receptors were chosen based on their association with the BDNF-NTRK2 pathway. The NTRK2 receptor has already been found to be altered in this sample population by our laboratory team previously.[44] Initially, ten different GABAergic receptors were chosen for examination. The Allan Brain Atlas was initially used to determine if transcripts for GABAergic receptors were present in the cingulate cortical region in humans using RNA transcripts through in-situ hybridization (ISH) on postmortem human brain tissue. While not conclusive, the ISH transcript cell morphology could be visualized through Nissl staining in the same cortical samples in the reference brain atlas. We eventually settled on three GABAergic receptors that had consistent expression levels that could be detected using serial dilutions of cells laser captured from the cingulate and were known to be affected by NTRK2/BDNF regulatory abilities. GABRA1 is downregulated by the JAK/STAT pathway that is downstream of NTRK2, GABRA4 is upregulated by the MAPK pathway also downstream of NTRK2, and GABBR1 is responsible for the G-protein coupled receptor function that allows GABA neurotransmitter to bind and activate. No significant differences were found for these three receptors. Both GABRA4 and GABBR1 did exhibit an upward expression trend albeit not significant. It is interesting to note that GABRA4 had extremely low expression levels in the control population. It is tempting to speculate that the gene was turned on during development of the disorder. Additional GABAergic genes were evaluated for expression levels in pyramidal cells excised from control donors but failed to exhibit reliable amplification and were excluded from the study. It might be beneficial to evaluate even those GABAergic receptors that were not reliably expressed in control tissue. They simply may be the low expressors while subjects with the disorder may have detectable expression levels. It is inconclusive at this early stage to state

that GABAergic receptors expression is not altered in ASD pyramidal cells. More information is needed including studies with different GABAergic receptors and a larger sample size to determine whether GABRA4 and GABBR1 are significantly different.

Simultaneous to laser capture studies, immunoblotting was performed to examine protein expression differences in BA10 and BA24 brain regions in ASD and TD donors for synaptic proteins that can impact GABAergic receptor expression and function. Some of these proteins have been shown to be differentially expressed in other brain areas. No differences were found in the cingulate cortex for any of the proteins examined in this study, even when adjusting for age or RIN correlations. We were unable to corroborate the downregulation found by Western blotting for PSD-95 or mTOR studies in the fusiform gyrus. In those studies mentioned, full length PSD-95 and mTOR were found to be reduced when analyzing 11 ASD and 13 TD controls in the fusiform gyrus which plays a role in object and facial recognition.[58] Our study was the first to examine spinophilin, CPLX, IGF1R and PARP1 protein expression in the cingulate cortex when comparing ASD to TD control donors as well as ASD in general. Unfortunately, all these proteins are expressed in multiple cell types at potentially high levels severely limiting the conclusions of these findings. Additional studies using immunohistochemistry to evaluate cell specific expression in pyramidal neurons and morphological analysis such as Golgi staining would give a more complete picture of specific GABAergic synaptic pathology in ASD.

Brain tissue that is received in our laboratory is matched by age and PMI. It was interesting that age correlations were present in five of the six proteins for immunoblotting with age in the control population in the ACC or BA24 but were not found in the frontal cortex or BA10 of the exact same donors. This result was not expected because research has shown developmental differences in gene expression from both BA10 and BA24. Not only expression differences but also the cellular makeup of brain tissue. It was shown in postmortem brain tissue of healthy individuals that as humans age the density of oligodendrocytes increases, which is

important in maintaining neuronal communication.[59] As the human brain develops multiple genes are found to have altered expression. This research has been performed on both males and females. While they found differences, the end result was the same: as the brain develops gene expression levels change.[60,61] Also, RIN correlations were found for four of the six proteins, but again were not found in BA10 nor were there any correlations between the three GABAergic genes examined with RIN. One thing to note, RIN has been shown to be a good indication of mRNA quantity but cannot predict mRNA integrity. With this knowledge researchers can say there is mRNA present in the postmortem tissue but cannot be sure the brain tissue is a good quality, and the mRNA has remained intact.[62]

Limitations

This study includes several limitations that must be taken into consideration. Experimentation was conducted with small samples sizes; however, in the ASD postmortem literature, a study number of 12 is considered large. Additionally, it was a targeted study for a focused number of synaptic proteins and genes to validate the current literature that is plagued with even smaller study numbers to evaluate synaptic pathology in BA24 and BA10 regions. Sadly, it was estimated by a leading postmortem research in the field at a recent conference that only 150 brains are in circulation for all the ASD postmortem studies in the literature. Additionally, the tissue pairs we received were also a range of ages from 4-37 which does not allow for development-specific analysis. We have early, adolescent, and adult neuronal development trajectories represented in our sample population. ASD considered to be a neurodevelopmental disorder; therefore, it would be ideal to study each developmental stage. ASD is also known as a spectrum disorder due to the heterogeneity of the symptoms. It has even been referred to as “autisms.”

CHAPTER 5. CONCLUSION

From previous published studies it is hypothesized that ASD has a multi-factorial etiology that culminates to cause the disease's behavioral phenotype. Researchers have been sequencing the genomes of ASD patients to compare against typically developing controls in hopes of finding a unique genetic etiology. However, these experiments have left more questions than answers. Clues of the etiology and future treatment targets may lie in studying the pathology of ASD. In these experiments, frozen brain regions BA24 and BA10 were used to analyze pyramidal neuron gene expression and tissue homogenate protein concentration that may be related to GABAergic expression. This study did not identify any significant differences between ASD or TD for either of the experiments in either of the brain regions. While there were trends in gene expression upregulation for two of the GABAergic receptor genes evaluated, they failed to make statistical significance. While this study did not conclusively identify GABAergic related pathology, it will help shape future studies for other targets of the NTRK2 pathway in human ASD pathology.

REFERENCES

1. Association AP. DSM-5 Autism Spectrum Disorder Fact Sheet. 2014;(October):233–255.

2. Maenner MJ, Shaw KA, Baio J, Washington A, Patrick M, DiRienzo M, Christensen DL, Wiggins LD, Pettygrove S, Andrews JG, et al. Prevalence of Autism Spectrum Disorder Among Children Aged 8 Years — Autism and Developmental Disabilities Monitoring Network, 11 Sites, United States, 2016. MMWR. Surveillance Summaries. 2020;69(4). doi:10.15585/mmwr.ss6904a1

3. CDC - Centers for Disease Control and Prevention. Data & Statistics on Autism Spectrum Disorder | CDC. CDC.gov. 2019 [accessed 2020 Apr 24]:1. https://www.cdc.gov/ncbddd/autism/data.html

4. Geschwind DH. Genetics of autism spectrum disorders. Trends in Cognitive Sciences. 2011;15(9):409–416. doi:10.1016/j.tics.2011.07.003

5. Bolton P, Macdonald H, Pickles A, Rios P, Goode S, Crowson M, Bailey A, Rutter M. A Case-Control Family History Study of Autism. Journal of Child Psychology and Psychiatry. 1994;35(5):877–900. doi:10.1111/j.1469-7610.1994.tb02300.x

6. Crowley JJ, Szatkiewicz J, Kähler AK, Giusti-Rodriguez P, Ancalade NE, Booker JK, Carr JL, Crawford GE, Losh M, Stockmeier CA, et al. Common-variant associations with fragile X syndrome. Molecular Psychiatry. 2019;24(3):338–344. doi:10.1038/s41380-018-0290-3

7. Constantino JN, Lajonchere C, Lutz M, Teddi Gray Anna Abbacchi B, Kathleen McKenna Deepti Singh M, Richard Todd BD. Article Autistic Social Impairment in the Siblings of Children With Pervasive Developmental Disorders. 2006.

8. Castellani CA, Arking DE. High-Risk, High-Reward Genetics in ASD. Neuron. 2020;105(3):407–410. doi:10.1016/j.neuron.2020.01.007

9. Clancy S. Copy Number Variation Learn Science at Scitable. 2008.

10. Meguro-Horike M, Yasui DH, Powell W, Schroeder DI, Oshimura M, LaSalle JM, Horike S ichi. Neuron-specific impairment of inter-chromosomal pairing and transcription in a novel model of human 15q-duplication syndrome. Human Molecular Genetics. 2011;20(19):3798–3810. doi:10.1093/hmg/ddr298

11. Warrier V, Baron-Cohen S, Chakrabarti B. Genetic variation in GABRB3 is associated with Asperger syndrome and multiple endophenotypes relevant to autism. Molecular Autism. 2013;4(1):1–11. doi:10.1186/2040-2392-4-48

12. Yoo HJ, Cho IH, Park M, Yang SY, Kim SA. Family based association of GRIN2A and GRIN2B with Korean autism spectrum disorders. Neuroscience Letters. 2012;512(2):89–93. doi:10.1016/j.neulet.2012.01.061

13. Drew CJG, Kyd RJ, Morton AJ. Complexin 1 knockout mice exhibit marked deficits in social behaviours but appear to be cognitively normal. Human Molecular Genetics. 2007;16(19):2288–2305. doi:10.1093/hmg/ddm181

14. Chang S, Reim K, Pedersen M, Neher E, Brose N, Taschenberger H. Complexin stabilizes newly primed synaptic vesicles and prevents their premature fusion at the mouse calyx of held synapse. Journal of Neuroscience. 2015;35(21):8272–8290. doi:10.1523/JNEUROSCI.4841-14.2015

15. Krumm N, O'Roak BJ, Karakoc E, Mohajeri K, Nelson B, Vives L, Jacquemont S, Munson J, Bernier R, Eichler EE. Transmission disequilibrium of small CNVs in simplex autism. American Journal of Human Genetics. 2013;93(4):595–606. doi:10.1016/j.ajhg.2013.07.024

16. Jeste SS, Tuchman R. Correction: Practice settings and dentists' job satisfaction (The Journal of the American Dental Association (2015) 146(8) (600–609) (S0002817715003475) (10.1016/j.adaj.2015.03.001)). Journal of the American Dental Association. 2017;148(11):787. doi:10.1016/j.adaj.2017.09.031

17. Zhou Y, Shi L, Cui X, Wang S, Luo X. Functional connectivity of the caudal anterior cingulate cortex is decreased in autism. PLoS ONE. 2016;11(3). doi:10.1371/journal.pone.0151879

18. Feng J, Yan Z, Ferreira A, Tomizawa K, Liauw JA, Zhuo M, Allen PB, Ouimet CC, Greengard P. Spinophilin regulates the formation and function of dendritic spines. Proceedings of the National Academy of Sciences of the United States of America. 2000;97(16):9287–9292. doi:10.1073/pnas.97.16.9287

19. Yoo KS, Lee K, Oh JY, Lee H, Park H, Park YS, Kim HK. Postsynaptic density protein 95 (PSD-95) is transported by KIF5 to dendritic regions. Molecular Brain. 2019;12(1):1–12. doi:10.1186/s13041-019-0520-x

20. Grant SGN. Synaptopathies: Diseases of the synaptome. Current Opinion in Neurobiology. 2012;22(3):522–529. http://dx.doi.org/10.1016/j.conb.2012.02.002. doi:10.1016/j.conb.2012.02.002

21. Zhu J, Shang Y, Xia C, Wang W, Wen W, Zhang M. Guanylate kinase domains of the MAGUK family scaffold proteins as specific phospho-protein-binding modules. EMBO Journal. 2011;30(24):4986–4997. doi:10.1038/emboj.2011.428

22. Wu LJ, Li X, Chen T, Ren M, Zhuo M. Characterization of intracortical synaptic connections in the mouse anterior cingulate cortex using dual patch clamp recording. Molecular Brain. 2009;2(1):1–12. doi:10.1186/1756-6606-2-32

23. Herbison AE, Moenter SM. Depolarising and Hyperpolarising Actions of GABAA Receptor Activation on Gonadotrophin-Releasing Hormone Neurones: Towards an Emerging Consensus. Journal of Neuroendocrinology. 2011;23(7):557–569. doi:10.1111/j.1365-2826.2011.02145.x

24. Khazipov R. GABAergic synchronization in epilepsy. Cold Spring Harbor Perspectives in Medicine. 2016;6(2):1–14. doi:10.1101/cshperspect.a022764

25. El-Ansary A, Al-Ayadhi L. GABAergic/glutamatergic imbalance relative to excessive neuroinflammation in autism spectrum disorders. Journal of Neuroinflammation. 2014;11(1):1–9. doi:10.1186/s12974-014-0189-0

26. Naaijen J, Bralten J, Poelmans G, Glennon JC, Franke B, Buitelaar JK, Faraone S, Asherson P, Banaschewski T, P Ebstein R, et al. Glutamatergic and GABAergic gene sets in attention-deficit/hyperactivity disorder: Association to overlapping traits in ADHD and autism. Translational Psychiatry. 2017;7(1):1–7. doi:10.1038/tp.2016.273

27. Al-Otaish H, Al-Ayadhi L, Bjørklund G, Chirumbolo S, Urbina MA, El-Ansary A. Relationship between absolute and relative ratios of glutamate, glutamine and GABA and severity of autism spectrum disorder. Metabolic Brain Disease. 2018;33(3):843–854. doi:10.1007/s11011-018-0186-6

28. Disorders I of M (US) F on N and NS. Overview of the Glutamatergic System. 2011.

29. Petroff OAC. GABA and glutamate in the human brain. Neuroscientist. 2002;8(6):562–573. doi:10.1177/1073858402238515

30. Vaccarino FM, Smith KM. Increased Brain Size in Autism-What It Will Take to Solve a Mystery. Biological Psychiatry. 2009;66(4):313–315. doi:10.1016/j.biopsych.2009.06.013

31. Courchesne E, Pramparo T, Gazestani VH, Lombardo M v., Pierce K, Lewis NE. The ASD Living Biology: from cell proliferation to clinical phenotype. Molecular Psychiatry. 2019;24(1):88–107. doi:10.1038/s41380-018-0056-y

32. Waterhouse L. Social cognition The Social Brain is a Complex Su- Social Brain. ScienceDirect. 2013.

33. Frith CD. The social brain? Philosophical Transactions of the Royal Society B: Biological Sciences. 2007;362(1480):671–678. doi:10.1098/rstb.2006.2003

34. Seghatol-Eslami VC, Maximo JO, Ammons CJ, Libero LE, Kana RK. Hyperconnectivity of social brain networks in autism during action-intention judgment. Neuropsychologia. 2020;137(June 2019):107303. doi:10.1016/j.neuropsychologia.2019.107303

35. Horder J, Petrinovic MM, Mendez MA, Bruns A, Takumi T, Spooren W, Barker GJ, Künnecke B, Murphy DG. Glutamate and GABA in autism spectrum disorder-a translational magnetic resonance spectroscopy study in man and rodent models. Translational Psychiatry. 2018;8(1):1–11. doi:10.1038/s41398-018-0155-1

36. Bathina S, Das UN. Brain-derived neurotrophic factor and its clinical Implications. Archives of Medical Science. 2015;11(6):1164–1178. doi:10.5114/aoms.2015.56342

37. Miranda M, Morici JF, Zanoni MB, Bekinschtein P. Brain-Derived Neurotrophic Factor: A Key Molecule for Memory in the Healthy and the Pathological Brain. Frontiers in Cellular Neuroscience. 2019;13. doi:10.3389/fncel.2019.00363

38. Gupta VK, You Y, Gupta VB, Klistorner A, Graham SL. TrkB receptor signalling: Implications in neurodegenerative, psychiatric and proliferative disorders. International Journal of Molecular Sciences. 2013;14(5):10122–10142. doi:10.3390/ijms140510122

39. Goetz T, Arslan A, Wisden W, Wulff P. GABAA receptors: structure and function in the basal ganglia. Progress in Brain Research. 2007;160:21–41. doi:10.1016/S0079-6123(06)60003-4

40. Duthey B, Caudron S, Perroy J, Bettler B, Fagni L, Pin J-P, Prézeau L. A Single Subunit (GB2) Is Required for G-protein Activation by the Heterodimeric GABA $_B$ Receptor. Journal of Biological Chemistry. 2002;277(5):3236–3241. doi:10.1074/jbc.M108900200

41. Terunuma M. Diversity of structure and function of GABAB receptors: A complexity of GABAB-mediated signaling. Proceedings of the Japan Academy Series B: Physical and Biological Sciences. 2018;94(10):390–411. doi:10.2183/pjab.94.026

42. Orlic-Milacic M. Reactome | BDNF activates NTRK2 (TRKB) signaling. 2018 [accessed 2020 May 18]. https://reactome.org/content/detail/R-HSA-9024909

43. Stephenson FA. Understanding the GABA(A) receptor: A chemically gated ion channel. Biochemical Journal. 1988;249(1):21–32. doi:10.1042/bj2490021

44. Chandley MJ, Crawford JD, Szebeni A, Szebeni K, Ordway GA. NTRK2 expression levels are reduced in laser captured pyramidal neurons from the anterior cingulate cortex in males with autism spectrum disorder. Molecular Autism. 2015;6(1):1–12. doi:10.1186/s13229-015-0023-2

45. Correia CT, Coutinho AM, Sequeira AF, Sousa IG, Lourenço Venda L, Almeida JP, Abreu RL, Lobo C, Miguel TS, Conroy J, et al. Increased BDNF levels and NTRK2 gene association suggest a disruption of BDNF/TrkB signaling in autism. Genes, Brain and Behavior. 2010;9(7):841–848. doi:10.1111/j.1601-183X.2010.00627.x

46. Ohira K, Hayashi M. A New Aspect of the TrkB Signaling Pathway in Neural Plasticity. Current Neuropharmacology. 2009;7(4):276–285. doi:10.2174/157015909790031210

47. Fahnestock M. Bridging the Gap between Genes and Behavior: Brain-Derived Neurotrophic Factor and the mTOR Pathway in Idiopathic Autism. Autism-Open Access. 2015;05(02). doi:10.4172/2165-7890.1000143

48. Conditions G. Genetics Home Reference MECP2 duplication syndrome. 2017.

49. Chapleau CA, Larimore JL, Theibert A, Pozzo-Miller L. Modulation of dendritic spine development and plasticity by BDNF and vesicular trafficking: Fundamental roles in neurodevelopmental disorders associated with mental retardation and autism. Journal of Neurodevelopmental Disorders. 2009;1(3):185–196. doi:10.1007/s11689-009-9027-6

50. Sheikh AM, Malik M, Wen G, Chauhan A, Chauhan V, Gong CX, Liu F, Brown WT, Li X. BDNF-Akt-Bcl2 antiapoptotic signaling pathway is compromised in the brain of autistic subjects. Journal of Neuroscience Research. 2010;88(12):2641–2647. doi:10.1002/jnr.22416

51. Jäkel S, Dimou L. Glial cells and their function in the adult brain: A journey through the history of their ablation. Frontiers in Cellular Neuroscience. 2017;11(February):1–17. doi:10.3389/fncel.2017.00024

52. Ghaffari MA, Mousavinejad E, Riahi F, Mousavinejad M, Afsharmanesh MR. Increased Serum Levels of Tumor Necrosis Factor-Alpha, Resistin, and Visfatin in the Children with Autism Spectrum Disorders: A Case-Control Study. Neurology Research International. 2016;2016. doi:10.1155/2016/9060751

53. Sciara A. Neuroinflammatory Gene Expression Increases in Anterior Cingulate Cortical White and Gray Matter of Males with Autism Specturm Disorder. 2017.

54. Ke Y, Wang C, Zhang J, Zhong X, Wang R, Zeng X, Ba X. The Role of PARPs in Inflammation-and Metabolic-Related Diseases: Molecular Mechanisms and Beyond. Cells. 2019;8(9):1–22. doi:10.3390/cells8091047

55. Jensen DM. 肌肉作为内分泌和旁分泌器官 HHS Public Access. Physiology & behavior. 2018;176(1):1570–1573. doi:10.1038/s41395-018-0061-4.

56. Crawford JD, Chandley MJ, Szebeni K, Szebeni A, Waters B, Ordway GA. Elevated GFAP Protein in Anterior Cingulate Cortical White Matter in Males With Autism Spectrum Disorder. Autism Research. 2015;8(6):649–657. doi:10.1002/aur.1480

57. Livak KJ, Schmittgen TD. Analysis of relative gene expression data using real-time quantitative PCR and the 2-ΔΔCT method. Methods. 2001;25(4):402–408. doi:10.1006/meth.2001.1262

58. Nicolini C, Ahn Y, Michalski B, Rho JM, Fahnestock M. Decreased mTOR signaling pathway in human idiopathic autism and in rats exposed to valproic acid. Acta neuropathologica communications. 2015;3:3. doi:10.1186/s40478-015-0184-4

59. Vostrikov V, Uranova N. Age-Related Increase in the Number of Oligodendrocytes Is Dysregulated in Schizophrenia and Mood Disorders. Schizophrenia Research and Treatment. 2011;2011:1–10. doi:10.1155/2011/174689

60. Berchtold NC, Cribbs DH, Coleman PD, Rogers J, Head E, Kim R, Beach T, Miller C, Troncoso J, Trojanowski JQ, et al. Gene expression changes in the course of normal brain aging are sexually dimorphic. 2008. www.pnas.org/cgi/content/full/

61. Colantuoni C, Hyde TM, Mitkus S, Joseph A, Sartorius L, Aguirre C, Creswell J, Johnson E, Deep-Soboslay A, Herman MM, et al. Age-related changes in the expression of schizophrenia susceptibility genes in the human prefrontal cortex. Brain Structure and Function. 2008;213(1–2). doi:10.1007/s00429-008-0181-5

62. Sonntag KC, Tejada G, Subburaju S, Berretta S, Benes FM, Woo TUW. Limited predictability of postmortem human brain tissue quality by RNA integrity numbers. Journal of Neurochemistry. 2016 Jul 1:53–59. doi:10.1111/jnc.13637

APPENDIX: Supplementary Information

Appendix Table 1. Thermocycler Steps cDNA and Pre-Amplification for All Genes.

Thermocycler Steps	1	2	3	4	5	6
cDNA	10 min, 25C	30 min, 50C	5 min, 85C	Hold, 1ul RNaseH	20 min, 37C	
GABBR1 (DT)	2 min, 95C	30 sec, 95C	15 sec, 67C	1 min, 72C Repeat 2-4 18X	5 min, 72C	Hold, 4C
18S rRNA (DT)	2 min, 95C	30 sec, 95C	15 sec, 53C	1 min, 72C Repeat 2-4 17X	5 min, 72C	Hold, 4C
GABRA4 (HS)	5 min, 95C	45 sec, 94C	25 sec, 69C	1 min, 72C Repeat 2-4 25X	10 min, 72C	Hold, 4C
Beta2Microglobulin (HS)	5 min, 95C	45 sec, 94C	2 sec, 52C	1 min, 72C Repeat 2-4 18X	10 min, 72C	Hold, 4C
GABRA1 (HS)	5 min, 95C	45 sec, 94C	50 sec, 65C	1 min, 72C Repeat 2-4 20X	10 min, 72C	Hold, 4C

Appendix Table 2. Primer Sequence and Accession Number

Target or Reference Gene	Primer Sequence	Genebank Accession Number
GABRA1	F- TGCCCATGCTTGCCCACTAA R- GACGTGATCCATCTTCTGCTACAACC	NM_001127645
GABRA4	F- GTGCAGAGAGAGAAGCATCCTGAAG R- TGGTTTCCCACCTCAGTTCTGTTG	NM_001204267
GABBR1	F- TCACTTCGACTCTGGACGACCT R- GGCACAGCTGGATCTGAGAAGAAA	NM_021903
18S Ribosomal RNA	F- GTAACCCGTTGAACCCCATT R- CCATCCAATCGGTAGTAGCG	NR_003286
Beta 2 Microglobulin	F- GACTTTGTCACAGCCCAAG R- GCAAGCAAGCAGAATTTGG	NM_004048

Appendix Table 3. Optimization Details for Preamplification of Primer Pairs.

Optimized Primers	Enzyme	Temperature	Cycles	cDNA Conc.	qPCR Temp
GABRA1	HotStar	65	20	Full	57
GABBR1	DreamTaq	67	18	Half	59
GABRA4	HotStar	69	25	Full	57
18S	DreamTaq	53	17	Forth	58
Beta2M	HotStar	52	18	Forth	57

Appendix Table 4. Master Mix Concentration Pre-Amp and qPCR

Target or Reference Gene	Pre-Amplification	RT-qPCR
GABRA1	H2O - 4.9 µl Enz - 6 µl Primer - 0.6 ul	H2O - 6.8 µl Enz - 9 µl Primer - 1.2 µl
GABRA4	H2O - 5.05 µl Enz - 6 µl Primer - 0.45 µl	H2O – 6.8 µl Enz - 9 µl Primer - 1.2 µl
GABBR1	H2O - 4.85 µl Enz - 6 µl Primer - 0.65 µl	H2O - 6.8 µl Enz - 9 µl Primer - 1.2 µl
18S Ribosomal RNA	H2O - 4.9 µl Enz - 6 µl Primer - 0.5 µl	H2O - 6.8 µl Enz - 9 µl Primer - 1.2 µl
Beta 2 Microglobulin	H2O - 5.05 µl Enz - 6 µl Primer - 0.45 µl	H2O - 6.9 µl Enz - 9 µl Primer - 1.1 µl

Appendix Table 5. Gene Selection and Reasoning

GABAa Receptor Subunits	Information
GABRA1	BDNF downregulates via JAK/STAT Pathway
GABRA4	BDNF upregulates via MAP Kinase Pathway
GABAb Receptor Subunits	
GABBR1	Essential for GPCR function

Appendix Table 6. Antibodies Used for Immunoblotting

Protein	Source	RRID#	Secondary Ab
Spinophilin*	Cell Signaling cat#14136S	AB_2572261	D-a-RabbitHRP
PSD-95*	Cell Signaling cat#3450S	AB_2292883	D-a-RabbitHRP
IGF1R*	Cell Signaling cat#3027S	AB_2122378	D-a-RabbitHRP
mTOR*	Cell Signaling cat#2983S	AB_2105622	D-a-RabbitHRP
Aggrecan*	Invitrogen cat#AHP0022	AB_2536346	S-a-MouseHRP
PARP1*	Cell Signaling cat#9532S	AB_659884	D-a-RabbitHRP
CPLX1*	Abcam ab231347	AB_2861372	D-a-RabbitHRP
GapDH*	EMD Millipore cat#MAB374	AB_2107445	S-a-MouseHRP
Sheep anti mouse IgG HRP+	GE Healthcare UK Limited cat#NA931V	AB_772210	
Donkey anti Rabbit IgG HRP+	GE Healthcare UK Limited cat#NA934V	AB_772206	

*indicates a primary antibody
+indicates secondary antibody

Appendix Table 7. Primary Antibody Overnight Incubation Solution

Protein	Solution
Spinophilin	6 mL 5% milk in PBS-Tween20 + 6 µL Spinophilin
PSD-95	6 mL 5% BSA in TBST + 6 µL PSD-9
IGF1R	6 mL 5% BSA in TBST + 6 µL IGF1R
mTOR	6 mL 5% BSA in TBST + 6 µL mTOR
Aggrecan	6 mL 5% BSA in TBST + 6 µL Aggrecan
PARP1	6 mL 5% milk in TBST + 6 µL PARP1
CPLX1	6 mL 5% milk in PBS-Tween20 + 6 µL CPLX1
GapDH	6 mL 5% milk in TBST + 1.2 µL GapDH

Appendix Table 8. Buffers for Western Blotting

Buffers	Components or Source
PBS 10X	Fisher Bioreagents- cat# BP3994
TE-Lysis	Fisher Scientific- (TrisHCl- EDTA)
Lameli (Loading)*	BioRad Laboratories- 4x Lameli Sample Buffer cat# 161-0747
10X Running Stock**	800mL distilled water, 30.4g Tris (Tris base), 144.2g Glycine, 10.0g of SDS. Volumize to 1L
10X Transfer Stock***	800mL distilled water, 30.3g Tris (Tris base), 144.1g Glycine. Volumize to 1L
Mild Stripping Buffer	15g Glycine, 1g SDS, 10mL Tween20, pH 2.2. Volumize to 1L
5% Milk Solution	1.25g of evaporated milk in 25 mL of PBS-Tween20

Note for T5:

**10% BME is added to the loading buffer to make 1X solution. An amount of 20 μL to 180 μL of loading buffer.*

***The running buffer used for gel electrophoresis is a dilution of the 10x stock. To prep the running buffer, obtain 100 mL of running buffer and dilute with 900 mL of distilled water. Place in the fridge as it needs to be cold before use.*

****For the transfer buffer used in transfer step, take 100 mL from the 10X stock, add 200 mL of methanol and then dilute with 700 mL of distilled water. Place in the fridge as it needs to be cold before use.*

Appendix Table 9. Cycle Optimization with HotStar Enzyme

69°C, 57° C w/ HotStar	11/05/2020
GABRA4	Threshold
12	25.56
16	20.87
20	17.14
24	15.35
Punch	18.13
Blank	37.23
+ Control	30.18

Appendix Table 10. cDNA Template Concentration Check for Threshold

69° C, 57° C w/ HotStar	3/08/2021
GABRA4	Threshold
Full	31.32
Half	31.83
Fourth	40.0
Punch	17.23
Blank	0
+ Control	28.91

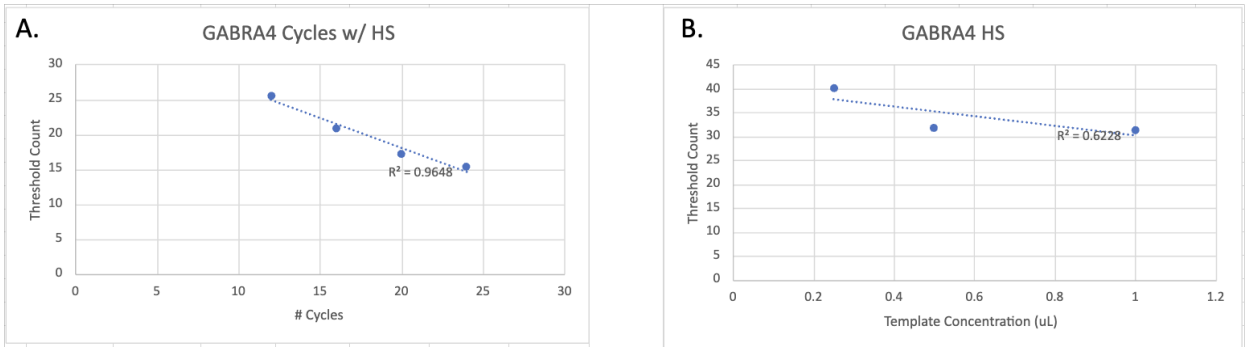

Appendix Figure 1. A) Graph of GABRA4 cycle optimization B) Graph of GABRA4 Template concentration check for threshold

Appendix Table 11. Cycle Optimization with HotStar Enzyme

67°C, 59° C w/ DreamTaq	1/24/2021
GABBR1	Threshold
14	25.25
18	22.58
F24	-
Punch	7.95
Blank	32.9
+ Control	20.02

Appendix Table 12. cDNA Template Concentration Check for Threshold

67° C, 59° C w/ DreamTaq	3/17/2021
GABBR1	Threshold
Full	18.73
Half	20.33
Fourth	21.06
Punch	13.66
Blank	36.52
+ Control	24.72

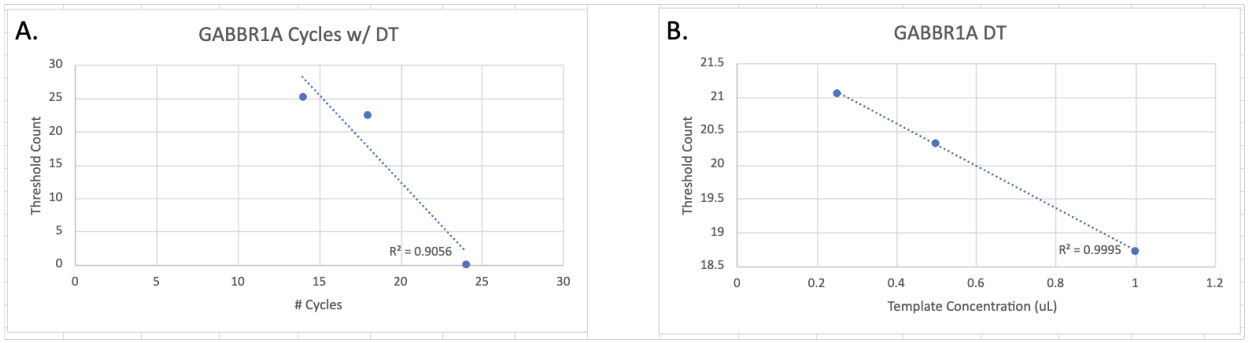

Appendix Figure 2. A) Graph of GABBR1 cycle optimization B) Graph of GABBR1 Template concentration check for threshold

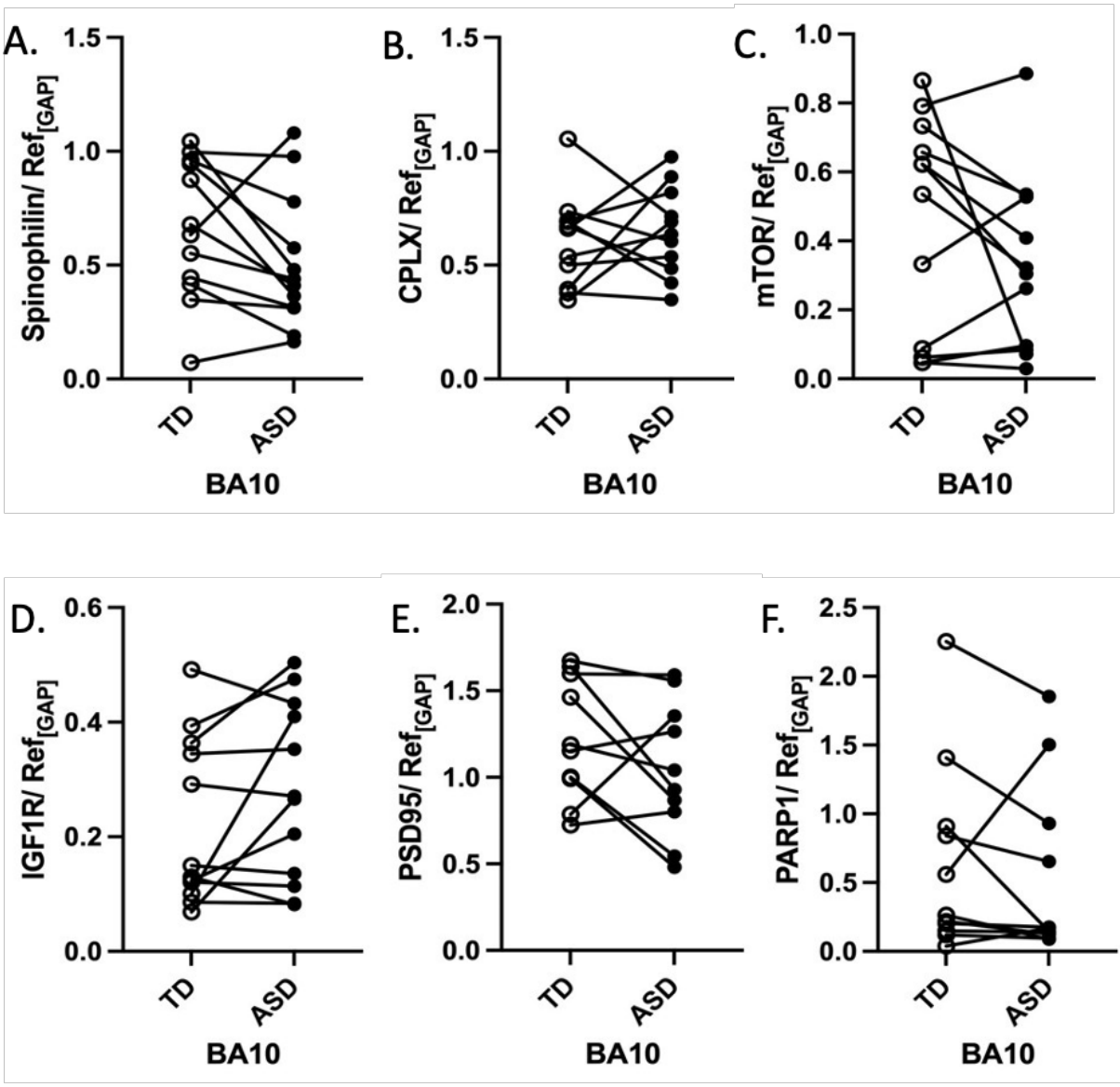

Appendix Figure 3. Panel A) Protein Expression of Spinophilin was determined by immunoblotting in human postmortem tissue from frontal cortex, BA10 (N=121), punch dissected brain tissue from TD control tissue and ASD tissue. Spinophilin protein expression was normalized to the protein expression of GAPDH. A paired Student's t-test was used to determine statistical significance of $p<0.05$. Panel B) PSD95 (N=10), Panel C) IGF1R (N=12), Panel D) mTOR (N=12), Panel E) CPLX1 (N=11), and Panel F) PARP1 (N=10).

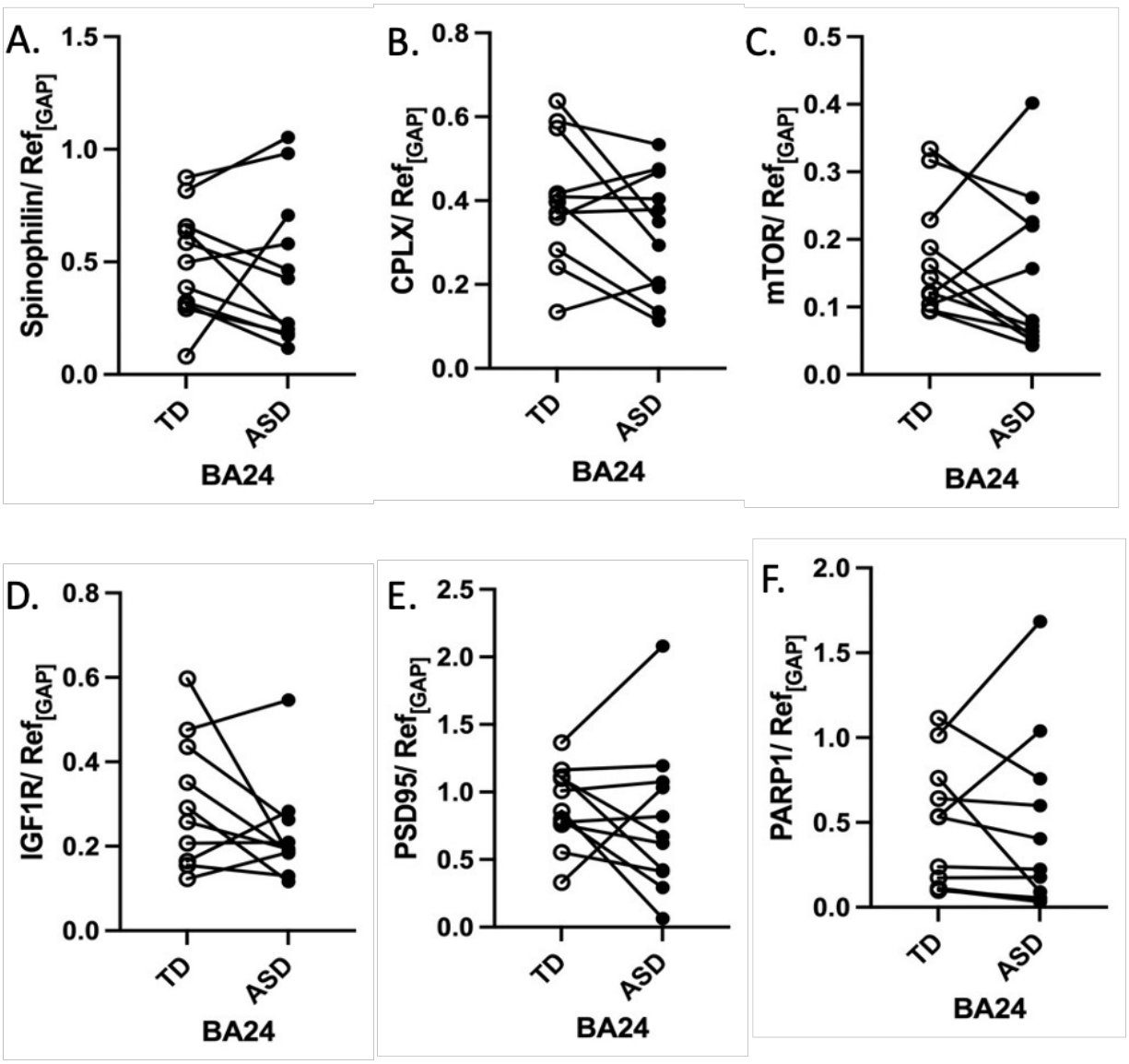

Appendix Figure 4. Panel A) Protein Expression of Spinophilin was determined by immunoblotting in human postmortem tissue from anterior cingulate cortex, BA24 (N=10~~1~~), punch dissected brain tissue from TD control tissue and ASD tissue. Spinophilin protein expression was normalized to the protein expression of GAPDH. A paired Student's t-test was used to determine statistical significance of $p<0.05$. Panel B) PSD95 (N=11), Panel C) IGF1R (N=10), Panel D) mTOR (N=11), Panel E) CPLX1 (N=11), and Panel F) PARP1 (N=10).

VITA

GETHEIN ANDREW

Education:	M.S. Biology, East Tennessee State University, Johnson City, Tennessee, 2021
	B.S. Health Sciences, East Tennessee State University, Johnson City, Tennessee, 2019
	William Blount High School, Maryville, Tennessee, 2015
Professional Experience:	Graduate Assistant, East Tennessee State University, College of Arts and Sciences, 2019-2021
	Laboratory Tech., East Tennessee State University, College of Public Health, 2016- 2019
Honors and Awards:	Graduate Assistantship, 2019-2021
	Appalachian Student Research Forum Winner, 2019
	Academic Performance Scholarship, 2015-2019